

Light-Dark FTIR Absorbance Difference Spectroscopy for the Study of Photosystem I

by

Andrew D. Davis

A THESIS SUBMITTED IN PARTIAL FULFILMENT OF
THE REQUIREMENTS FOR THE DEGREE OF

BACHELOR OF SCIENCE

in

The Faculty of Mathematics and Sciences

Department of Physics



BROCK UNIVERSITY

May 14, 2007

2007 © Andrew D. Davis

In presenting this thesis in partial fulfilment of the requirements for an advanced degree at the Brock University, I agree that the Library shall make it freely available for reference and study. I further agree that permission for extensive copying of this thesis for scholarly purposes may be granted by the head of my department or by his or her representatives. It is understood that copying or publication of this thesis for financial gain shall not be allowed without my written permission.

(Signature) _____

Department of Physics

Brock University
St.Catharines, Canada

Date _____

Abstract

It was supposed that the FTIR light-dark absorbance difference spectra of Gary Hastings and Jacques Breton could be duplicated. Light-dark absorption difference spectra of PS I particles derived from cyanobacteria were expected to show some signal, and promising results were obtained. The light-dark signal in the best difference spectrum obtained cannot be considered reliable, however, because the the dark-dark difference spectrum showed a larger absorption, and noise of comparable amplitude.

Contents

Abstract	ii
Contents	iii
List of Tables	v
List of Figures	vi
Acknowledgements	vii
1 Introduction	1
1.1 Photosynthesis	1
1.1.1 Fundamentals	1
1.1.2 Structure of the Photosynthetic Apparatus	2
1.1.3 Divisions of the Photosynthesis Process	3
1.1.4 Photochemistry	4
1.1.5 Photosystem I Structure	5
1.1.6 Dark Biochemistry	7
1.2 FTIR	9
1.2.1 IR Absorbance	9
1.2.2 IR Spectra	10
1.2.3 The Spectrometer	11
1.3 Expected Results	12
2 Methods	15
2.1 The Light Source and Detector	15
2.2 Photosystem I Samples	15
2.3 Generation of the Spectra	16
2.4 Problems and Solutions	16
2.4.1 Water Absorption	17
2.4.2 Sample Holder Material	17
2.4.3 Air Absorptions	24
2.4.4 Actinic Light Source Intensity	26
2.4.5 Signal Variance	26
2.4.6 Signal Averaging	27
2.4.7 Final Sample Holder	28
3 Light-Dark Difference Spectra	29
3.1 Polypropylene Slide Sample Holder	29
3.2 CaF ₂ Sample Holder Without Spacer	30

3.3 Final Sample Holder	31
4 Conclusions and Future Work	34
A Sample Physica Macro	36
B Table of Absorptions	39
Bibliography	40

List of Tables

2.1	Approximate Chlorophyll Concentration of Prepared Samples	16
3.1	Order of Gathered Spectra	31
B.1	Compilation of Identified IR Bands	39

List of Figures

1.1	Cross Section of a Leaf	2
1.2	3D Representation of a Chloroplast	3
1.3	The Z-Scheme	4
1.4	Thylakoid Membrane	5
1.5	Chlorophyll Molecule	6
1.6	PS I Reaction Centre	7
1.7	Phylloquinone Molecule	8
1.8	Simplified Chloroplast View	8
1.9	Electric Dipole Motion During Absorption	10
1.10	Typical Fourier Transform Spectrometer	12
1.11	Hastings' PS I Light-Dark Absorption Difference Spectrum	13
1.12	Breton's PS I Light-Dark Absorption Difference Spectrum	14
2.1	Chemical Structure of Polypropylene	17
2.2	Polypropylene Absorption Spectrum	18
2.3	PS I in Polypropylene Envelope Absorption Spectrum	19
2.4	PS I on Polypropylene Slide Absorption Spectrum	21
2.5	KBr Absorption Spectrum	22
2.6	Optical Properties of KBr	22
2.7	PS I in KBr Sample Holder Absorption Spectrum	23
2.8	Optical Properties of CaF ₂	24
2.9	CaF ₂ Absorption Spectrum	25
2.10	Laboratory Air Absorption Spectrum	25
2.11	Light-Dark Spectrum Showing Signal Variance	27
2.12	Final Experimental Apparatus	28
3.1	PS I on Polypropylene Slide Light-Dark Difference Spectrum	29
3.2	1000 Scan PS I Light-Dark Difference Spectra	30
3.3	30000 Scan PS I Light-Dark Difference Spectra	32
3.4	30000 Scan Power Spectrum of PS I Sample	32
3.5	30000 Scan PS I Light-Dark Spectra – Closer View of light-dark1	33
3.6	30000 Scan PS I Light-Dark Spectra – Viewed to 1200 cm ⁻¹	33
4.1	Hastings PS I Spectrum Including Dark-Dark Reference	34
4.2	PS II Visible Absorbance Spectrum	35

Acknowledgements

The first thanks goes to my wife, Mollie - a source of strength.

Dr. David Crandles was an excellent supervisor, both helpful and challenging. He pushed me and left me alone at all the right times.

Dr. Art van der Est is to be acknowledged for his willingness to share his time, his proof-reading skills and his astonishing knowledge of PS I and photosynthesis in general. Any biochemistry errors committed herein are mine alone, however.

Sudhakar Gunuganti was very helpful in the lab, and the design process, since he had the insight of practical experience. Baochang Liu is also to be thanked for sharing my serious squash addiction.

The rest of the Brock physics department also deserve my sincere thanks, all of whom are generous with their time.

Chapter 1

Introduction

This project used Fourier Transform Infrared Spectroscopy (FTIR) to study photosystem I (PS I) particles derived from cyanobacteria. This chapter will introduce the fundamentals of photosynthesis with a focus on cyanobacteria, to explain the composition and function of the PS I particles that were studied. The principles of FTIR spectroscopy and the results expected from the spectra will also be described.

1.1 Photosynthesis

Photosynthesis is a broad topic that can be approached from any of biology, chemistry, or physics. It is also important to our world - most of our useful energy (in forms like food and fossil fuels) comes directly or indirectly from photosynthesis[23]. Furthermore, ancient ancestors of cyanobacteria greatly influenced Earth's atmosphere, increasing the oxygen levels and making animal life possible.[15]

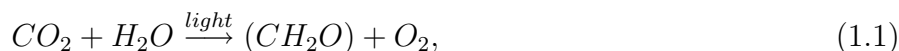
Photosynthesis, however, is not fully understood, and is an active field of research. An understanding of photosynthesis could lead to important developments, such as improvements in agriculture and light harvesting devices for energy. FTIR studies on PS I particles contribute to the understanding of the structure of the photosynthetic apparatus.[12, 13, 3, 4, 2]

1.1.1 Fundamentals

Photosynthesis is the process of capturing light energy and using electron transport to store it as chemical energy. The process can be either oxygenic or non-oxygenic, depending on the electron source used. Non-oxygenic photosynthesis, which will not be discussed here, uses H_2S or organic molecules as the electron source, and is carried out by purple and green bacteria. Oxygenic photosynthesis, which uses H_2O as a source of electrons, will be discussed in detail in this section. This type of photosynthesis occurs in the cells of plants, algae, cyanobacteria, and prochlorophytes (close relatives of cyanobacteria)[15]. Cyanobacteria are still sometimes referred to as blue-green algae, although they are a bacteria, not algae, and their colour ranges from blue-green to violet-red.

Almost all of the photosynthetic apparatus in cyanobacteria is the same as that of plants, and "the mechanism of cyanobacterial photosynthesis is identical to that of photosynthetic eukaryotes." [15] Thus, the discussion of photosynthesis in plants also applies to cyanobacteria, and research done on cyanobacteria is enlightening for plants as well. The popular endosymbiotic hypothesis postulates that the photosynthetic apparatus in plants evolved because of an early symbiotic relationship between plants and cyanobacteria. Cyanobacteria are used in research because they are easier and less time consuming to grow.

The familiar photosynthetic equation is



where (CH_2O) is a carbohydrate, such as $C_6H_{12}O_6$ - glucose. Equation 1.1 may be useful as an overview of photosynthesis, but doesn't correspond to any single process that occurs in nature. In

reality, many reaction steps are involved. This equation, however, reveals the reason photosynthesis is useful - it converts the sun's energy into chemical forms that can be used by plants and animals.

1.1.2 Structure of the Photosynthetic Apparatus

In plant leaves, photosynthesis occurs in the palisade and spongy mesophyll cells. These cells contain chloroplasts, the organelles responsible for photosynthesis. The chloroplasts are shown as black bodies around the periphery of the cells in Figure 1.1. The cells also contain a large central vacuole.

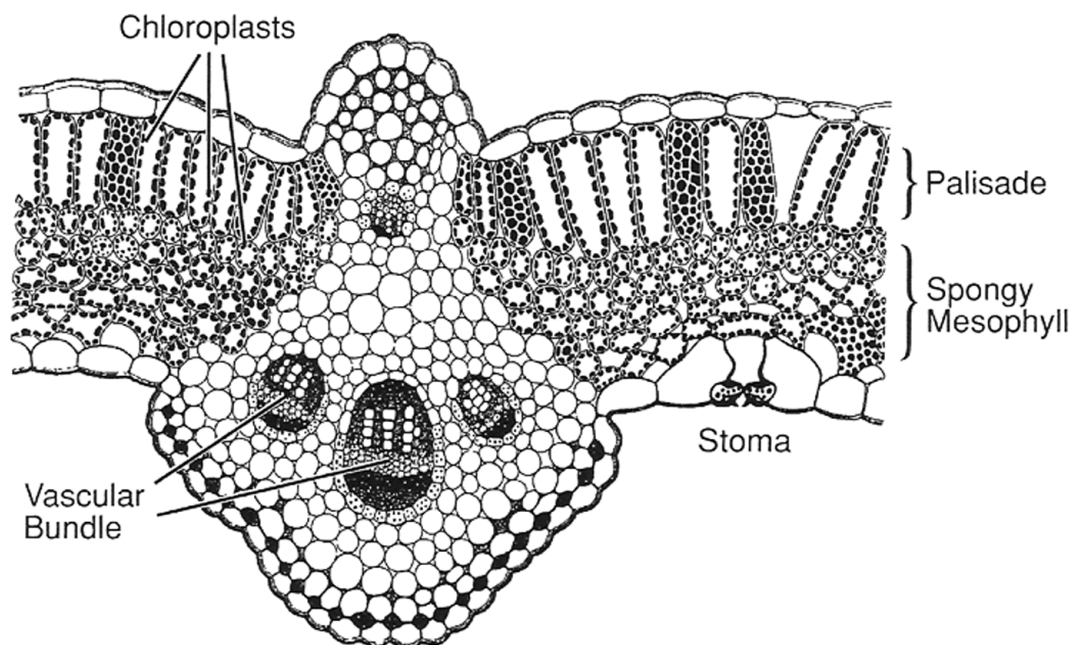


Figure 1.1: **Cross Section of a Leaf.** Chloroplasts are shown as black bodies, and there are spaces between the cells to permit free circulation of air entering through the stomata.[23]

The chloroplast is an organelle with a double outer envelope, as shown in Figure 1.2. It contains the photosynthetic apparatus. Chloroplasts contain an aqueous liquid called the stroma, and a single, deeply folded membrane called the thylakoid. The thylakoid membrane contains all of the chlorophyll molecules, and the electron transport systems involved in the photochemistry. The inside of the thylakoid membrane is called the lumen. The thylakoids of higher plants and algae contain different regions, with folded sections called grana connected by straight sections called stromal lamellae. The thylakoid membranes of cyanobacteria, however, do not contain granal and stromal sections.

Algae contain chloroplasts, but cyanobacteria contain no membrane-bound organelles and thus no chloroplasts. In cyanobacteria the thylakoid lies free within the single cell of the organism, where photosynthesis occurs. One of the only differences between photosynthesis in plants and cyanobacteria is the light gathering apparatus used by the organisms, called their antennae structures. Cyanobacteria have phycobilisomes (PBS's - a pigment-protein complex) attached to the thylakoid membrane, whereas higher plants and algae have a light harvesting protein complex integrated into the chloroplast membrane.[15]

The important point is that the photosynthetic apparatus in cyanobacteria is extremely similar to that of chloroplasts, and the chemical process that occurs is identical.

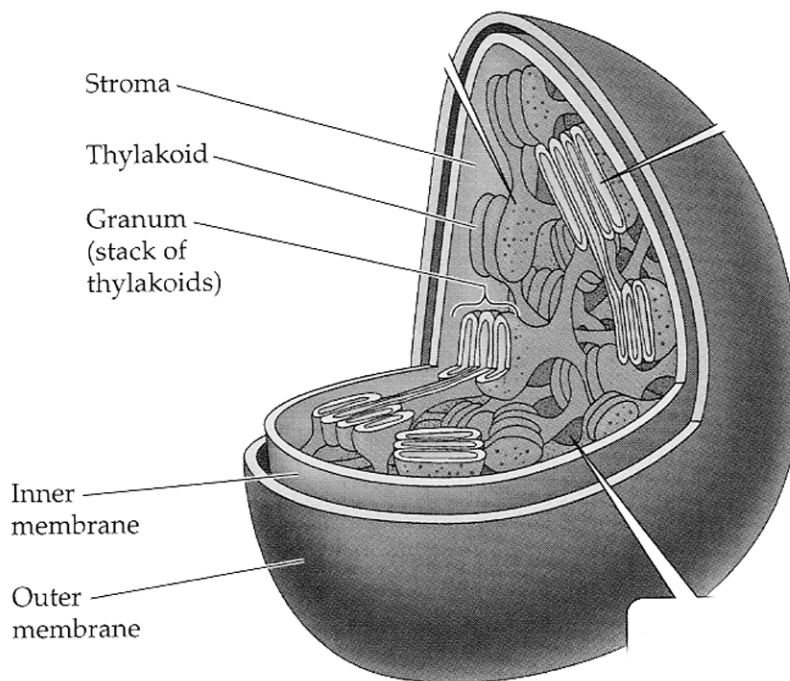
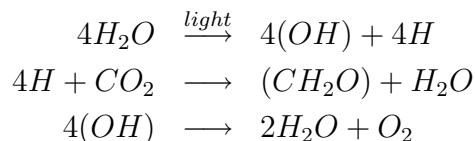


Figure 1.2: **3D Representation of a Chloroplast.** The heavily folded thylakoid membrane is shown. In cyanobacteria, the thylakoid is not bound by a chloroplast membrane.[17]

1.1.3 Divisions of the Photosynthesis Process

The overall arc of photosynthesis can be thought of as a transport of electrons from water to carbon dioxide, in order to reduce the carbon dioxide and form starches and sugars. Note that water is the source of O_2 in photosynthesis, not carbon dioxide - and the two steps are separate.

Early studies of photosynthesis revealed that equation 1.1 could be formally broken up into three stages[23]:



So light energy is used in the first step to divide water, and the other reactions don't explicitly require light. Also, it is now more clear that the CO_2 consumption and O_2 evolution steps are separate.

A simple experiment can illustrate this. When chloroplasts are separated from leaf tissue using centrifugation, the chloroplasts evolve oxygen when electron acceptors (oxidants) are added and the suspension is illuminated, but no CO_2 is consumed. Many quinones and dyes can be reduced by illuminated chloroplasts. This process is a transfer of electrons from water to organic and inorganic oxidants, and proves that O_2 evolution and CO_2 reduction are separate in photosynthesis.[11]

Photosynthesis can be broadly divided into two parts: *photochemistry* and *dark biochemistry*. The photochemistry involves the splitting of water, the transport of an electron to NADP, and the generation of energy rich molecules such as ATP. The dark biochemistry involves the reduction of carbon dioxide to make starches, powered by the energy rich molecules.

1.1.4 Photochemistry

The photochemistry occurs mostly in the folded thylakoid membranes, shown in Figure 1.2. The photochemical process is a series of redox reactions that splits water at the luminal face of the thylakoid, and transmits an electron to the molecule NADP. The overall redox potential difference through the process is about 1.6 V.[21] ATP, a major source of chemical energy for later reactions, is also formed during this process. The photochemistry is described by the so-called z-scheme, shown in Figure 1.3.

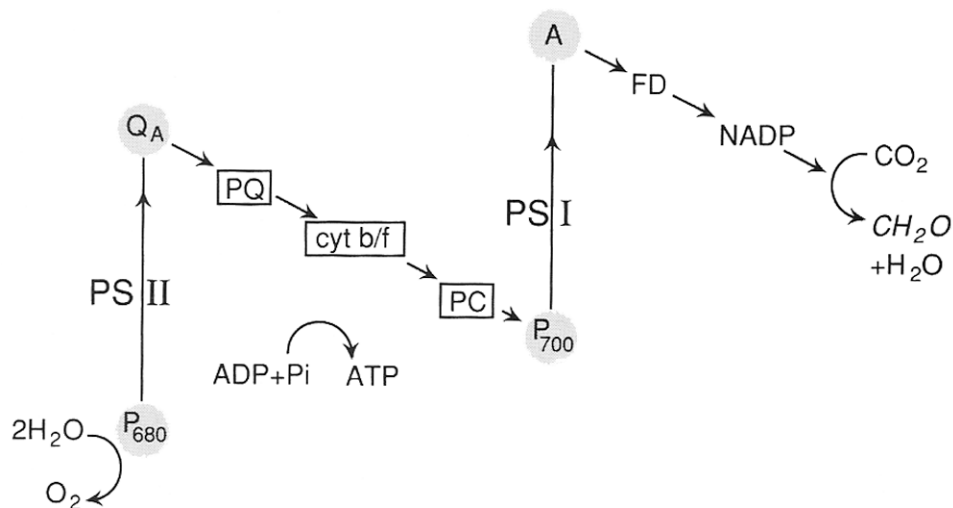


Figure 1.3: **The Z-Scheme.** The principle molecules in the electron transport from water to NADP are shown. The vertical axis of the figure represents increasing energy.[23]

The Figure shows P_{700} and P_{680} , which are the pigments of photosystem I and II, respectively, where light energy is transferred to electrons. The lowest energy absorbances of P_{700} and P_{680} occur at 700 nm and 680 nm, respectively. If light is absorbed by a chlorophyll molecule in the vicinity of PS II, the excitation energy (sometimes called an exciton) is transmitted between chlorophyll molecules until it reaches P_{680} . This energy is enough to reduce the permanently bound plastoquinone electron acceptor, Q_A , via several intermediates that are not shown in Figure 1.3. Subsequent redox reactions transfer the electron until it reaches PS I. The intermediate molecules that pass the electron are a mobile plastoquinone, the cytochrome b_6f complex and plastocyanin.

At PS I, P_{700} may be oxidized by the energy of a photon that was captured by a nearby chlorophyll molecule. A plastocyanin molecule may then reduce P_{700}^+ . The electron is again passed through a series of intermediate redox reaction steps until it reaches NADP, or Nicotinamide adenine dinucleotide phosphate. NADP then becomes $NADPH_2$ (also written as $NADPH + H^+$). The intermediate molecule labelled FD in Figure 1.3 is ferredoxin, a soluble protein containing two iron-sulfur clusters.

The hole created at P_{680} is filled by the water splitting process



which liberates four electrons and deposits four protons in the lumen. Protons are *transported* to the lumen when plastoquinone, having accepted two electrons, picks up two H^+ ions from the stroma and deposits them in the lumen.

As a result of the water splitting process and the action of plastoquinone, H^+ ions build up in the lumen. The resulting proton gradient across the thylakoid membrane is discharged by ATPsynthase to form the energy rich molecule ATP from ADP and phosphate (phosphate is written as Pi in Figure 1.3, for inorganic phosphate.) ATPsynthase is shown in Figure 1.4 as CF_0 and CF_1 .

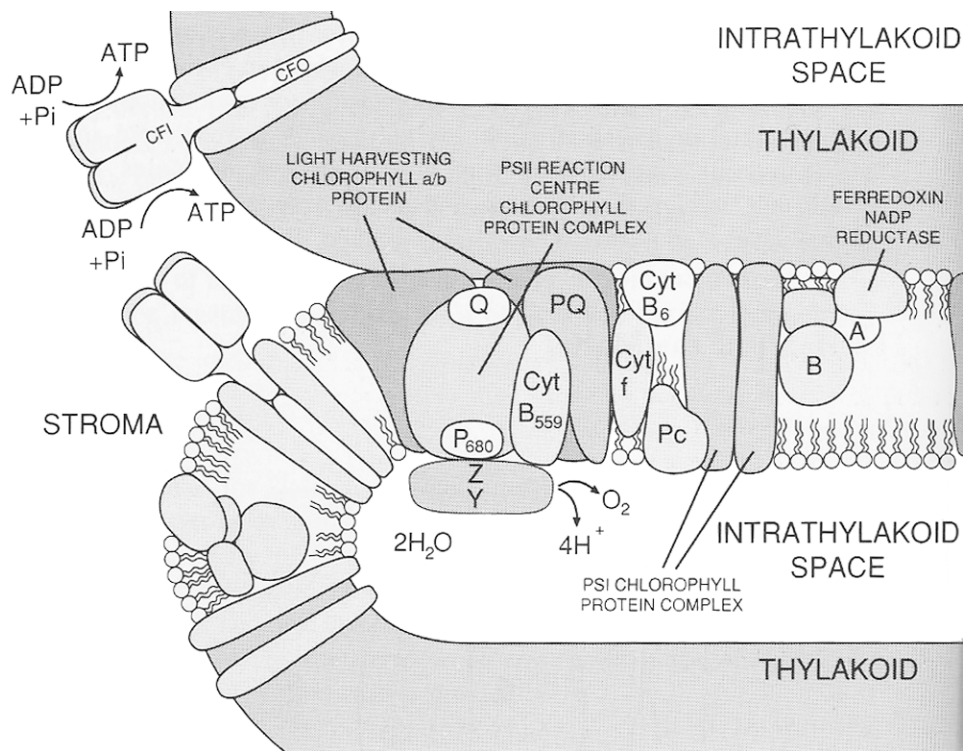


Figure 1.4: **Thylakoid Membrane.** A schematic view of the thylakoid membrane, showing the water splitting that causes the H^+ gradient to build up.[23]

Eight photons are normally required to complete the z-scheme per molecule of O_2 (four electrons produced during water splitting times two reaction centre excitations). Sometimes the electron can cycle through PS I and cytochrome b_6f , however, which generates ATP and increases the average requirement of photons from eight toward nine, as seen experimentally.

Pseudocyclic electron transport can also occur, in which the electron is finally accepted by oxygen, and hydrogen peroxide forms. This means that there is no net production of oxygen and NADP is not reduced. Pseudocyclic electron transport may seem useless, but the energy rich molecule ATP is produced, which is useful for later reactions. It is thought that linear electron transport, the process that reduces NADP, occurs much more than cyclic and pseudocyclic electron transport.[23]

In a leaf or cyanobacteria, then, the effect of the photochemistry is the donation of an electron from water to NADP. In experiments, however, both artificial electron donors and acceptors are often used, and individual pieces of the photosynthetic apparatus may be separated and investigated.

1.1.5 Photosystem I Structure

PS I is surrounded by a large number of chlorophyll molecules, and there are two chlorophyll-a molecules at its centre, forming P_{700} . A representation of the chlorophyll molecule is shown in Figure 1.5. Notable features include the disk-like portion of the molecule, called a porphyrin, and the long carbon chain. Also note the three $C=O$ carbonyl groups.

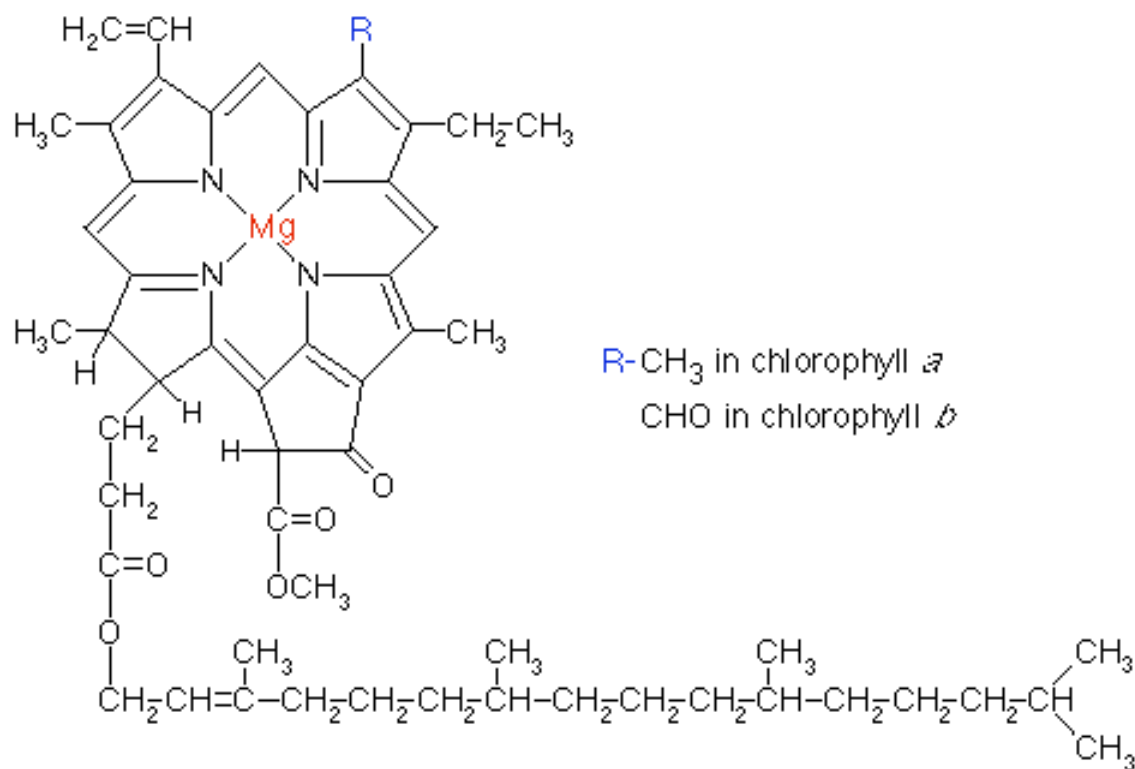


Figure 1.5: **Chlorophyll Molecule.** The disk-like portion of the molecule with a magnesium atom at its centre is called a porphyrin. The three carbonyl groups present were important in this project.

The PS I structure has been determined by crystallography. Figure 1.6 represents the PS I reaction centre, with two chlorophyll molecules (viewed edge-on) at the centre of the image making up P_{700} . The two arms of electron acceptor molecules spiral out, where A_1 is the molecule phylloquinone. F_x , F_A and F_B are iron-sulfur clusters.

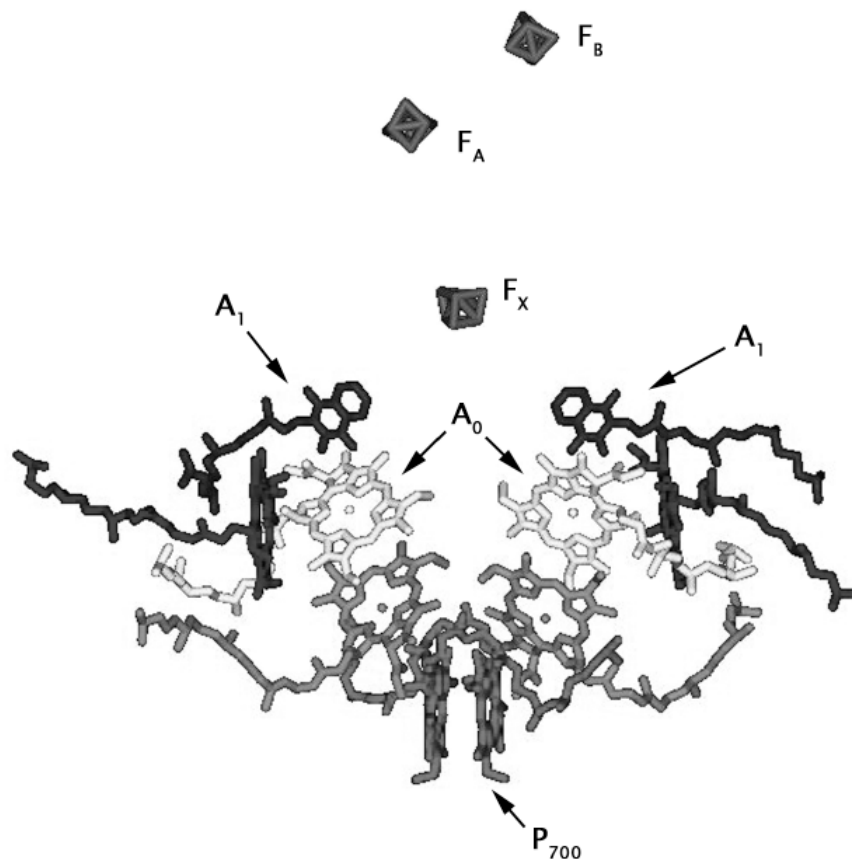


Figure 1.6: **PS I Reaction Centre.** The principle molecules of the reaction centre are shown. The two chlorophyll molecules (viewed edge-on) at the centre of the image make up P_{700} . The two arms of electron acceptor molecules spiral out, where A_1 is the molecule phylloquinone. F_x , F_A and F_B are iron-sulfur clusters.

A representation of the molecule phylloquinone (A_1 in the PS I reaction centre) is shown in Figure 1.7. The quinone group is the carbon ring with two attached carbonyls. These carbon-oxygen bonds were expected to form a large part of the light-dark signal in the difference spectra.

1.1.6 Dark Biochemistry

Despite its name, the dark biochemistry occurs mostly in the presence of light. Although the process does not directly use photons, many of the catalysts are light activated.[11] During the dark biochemistry, which occurs partly inside and partly outside of the chloroplast, ATP and $NADPH_2$ are used as energy sources. Inside the chloroplast, carbon dioxide is fixed and triose phosphate and starch form. Some triose phosphate leaves the chloroplast via the phosphate translocator, and sugar is formed. The process is shown in Figure 1.8.

The regulation mechanism of the phosphate translocator is not fully understood.

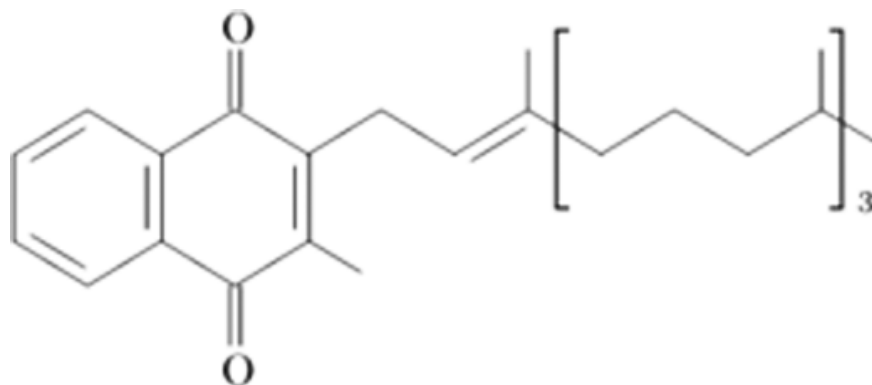


Figure 1.7: **Phylloquinone Molecule.** Most noteworthy for our discussion are the two carbonyl groups.

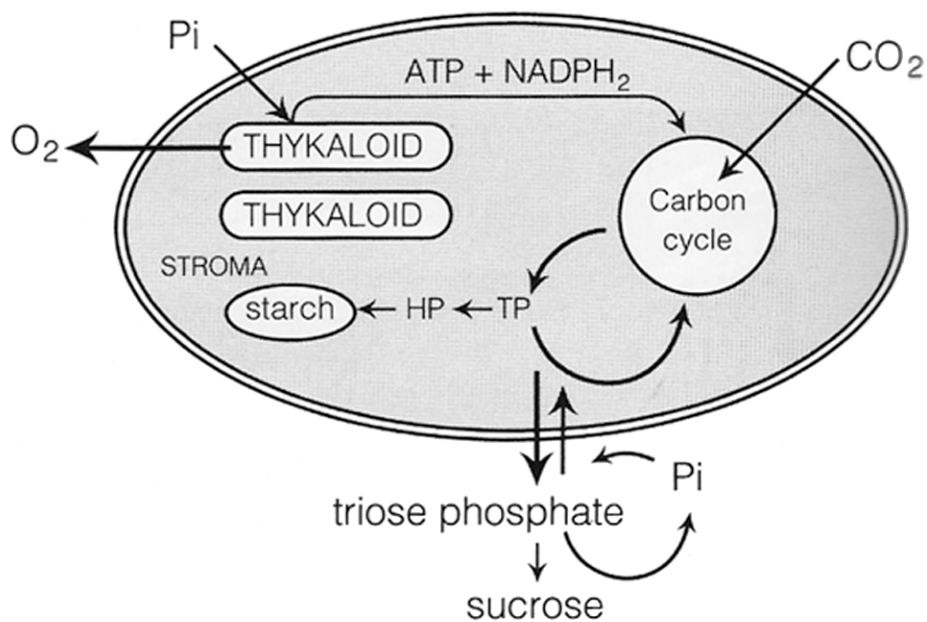
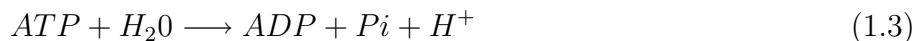


Figure 1.8: **Simplified Chloroplast View.** A functional view of the chloroplast, showing chemical reactions that occur inside and outside the chloroplast.[23]

Note that ATP donates energy to a reaction by being transformed:



The reverse reaction also occurs, requiring an energy input. This energy can come from the ΔpH that develops across the thylakoid membrane.

1.2 FTIR

An infrared (IR) spectrum is formed by measuring the wavelength dependence of the absorbance of infrared light by a sample. To avoid errors due to fluctuations in the source intensity, the light passed through a sample is compared to a reference without the sample present. The sample absorbs light at particular frequencies, while others are transmitted.

In “IR Spectroscopy: An Introduction”, Günzler and Gremlich explain the usefulness of FTIR as follows: “Like a fingerprint of a person, the IR spectrum is highly characteristic for a substance and can be used for identifying it. The high specificity is based on the good reproducibility with which the coordinates of the absorption maxima (generally, wavenumber and transmittance) can be measured.” [10]

Different chemical bonds absorb at different frequencies, so chemical processes can be observed by looking for different absorptions. If PS I is being studied, for example, a new feature in the spectrum after the sample is excited by light could mean that the phyloquinone electron acceptor has been reduced.

1.2.1 IR Absorbance

To explain the source of IR absorbance, it is useful to consider a diatomic molecule. The molecule can be modeled as a two mass system connected by a spring. In mechanics, the resonant frequency of vibration, ν , of such a system is given by

$$\nu = \frac{1}{2\pi} \sqrt{\frac{k}{\mu}}, \quad (1.4)$$

where k is the spring constant (a measure of the stiffness) and μ is the reduced mass, given by

$$\mu = \frac{m_1 m_2}{m_1 + m_2}. \quad (1.5)$$

Referring to the diatomic molecule, the quantity analogous to the spring force constant is bond strength. This means that the resonant frequency increases with bond strength, and is lower for larger masses. [9]

In reality most molecules would be modelled as a series of anharmonic oscillators with multiple natural vibration frequencies. While the molecule is irradiated by a spectrum of frequencies, it only absorbs at those matching the resonant cases. The intensity of the absorption depends on change in the dipole moment of the molecule.

The dipole moment forms since the atoms on either side of a bond tend to attract the electron forming the bond by different amounts. This can be thought of as creating small amounts of excess charge on the atoms, positive on one, negative on the other. The electric field of a passing photon causes opposing forces on the two ends of the electric dipole, and induces an oscillation, as shown in Figure 1.9. [6]

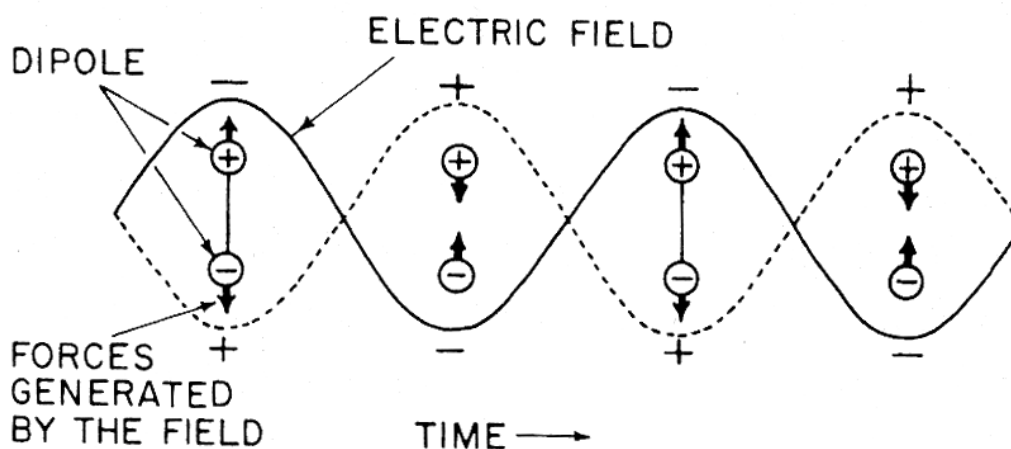


Figure 1.9: **Electric Dipole Motion During Absorption.** The motion of atoms on either end of a polar bond when infrared light is absorbed.[6]

Historically, many spectra have been performed on known substances. By examining and comparing the results, some of the bands produced on a typical absorbance spectrum can be qualitatively assigned to the motion of particular bonds in the substance being studied. Molecular vibrations can take different forms, such as symmetric and asymmetric stretching, bending in the plane and out of the plane of the molecule, and rocking in various ways.[9]

1.2.2 IR Spectra

An IR spectrum is usually expressed in terms of wavenumber, rather than wavelength. Wavenumber is often given the symbol $\tilde{\nu}$, and is calculated as the reciprocal of wavelength, as shown in equation 1.6. The units normally used for wavenumber are cm^{-1} .

$$\tilde{\nu} = \frac{1}{\lambda} \quad (1.6)$$

By examining the intensity of light passing through the sample at each wavenumber, a transmission spectrum can be produced, according to equation 1.7. This is a dimensionless quantity.

$$T_{\tilde{\nu}} = \frac{I}{I_0} \quad (1.7)$$

I represents the light intensity after passing through the sample, and I_0 represents the intensity without passing through the sample. In practice, however, I_0 must be taken in a separate step as a reference spectrum without the sample present.

Published works on FTIR studies of photosynthesis normally refer to units of absorbance at a particular wavenumber, rather than transmission. Transmission data can be converted to absorbance using equation 1.8. Absorbance is also dimensionless.

$$A_{\tilde{\nu}} = -\log(T_{\tilde{\nu}}) = \log\left(\frac{I_0}{I}\right) \quad (1.8)$$

Some may find absorbance plots less intuitive than transmission ones, but it may help to note that absorbances of 1.0 and 2.0 represent 10% and 1% of incident light passing through the sample, respectively.

Absorbance is often used in chemistry related applications of spectroscopy because it is a direct relation to sample concentration. Absorbance can be expressed in terms of the Beer-Lambert law as $A = alc$, where a is the so-called absorptivity, l is the sample thickness, and c is the sample concentration. The absorptivity is characteristic of a particular substance at a particular wavelength. It may also be expressed as molar absorptivity, ϵ . [18, 9]

Often the vertical axis of a spectrum will be labelled with ΔA , which is produced by subtracting two absorbance spectra. Another quantity sometimes used is the optical density, defined as absorbance divided by the sample thickness, as in equation 1.9.

$$OD_{\tilde{\nu}} = \frac{A_{\tilde{\nu}}}{l} \quad (1.9)$$

Likewise, the quantity ΔOD sometimes appears as a spectral label to indicate the difference of two optical density spectra.

For each band displayed on an absorbance difference or ΔOD spectrum, an upward and downward form should appear. This occurs because reducing phyloquinone, for example, changes the C=O bond strength. This causes the absorbance band corresponding to this bond to shift in energy, and thus appear at different positions in the two spectra subtracted to form the Δ Absorbance one.

1.2.3 The Spectrometer

Fourier transform infrared spectroscopy is slightly different than conventional infrared spectroscopy, and has several advantages. A diffraction grating is used in a conventional spectrometer to physically separate the different wavelengths of light. Each wavelength is then passed through the sample in turn, and the light intensity is recorded for each wavelength at the available resolution.

In FTIR, all wavelengths of light are recorded at the same time, but a Michelson interferometer is placed in the path of the incident light, as in Figure 1.10. The interferometer splits the incident light into two paths and then recombines it. The light on one path has a fixed distance to travel, while the other path includes a movable mirror that varies the path distance travelled by the light. The resulting signal depends on the path difference of the two arms of the interferometer. For any given wavelength of light, if the path difference between the two arms is a multiple of $\frac{1}{2}\lambda$, the light constructively interferes and the signal intensity increases. If the path difference is an odd multiple of $\frac{1}{4}\lambda$, the light from the two arms will completely destructively interfere. As the mirror is moved, it will repeatedly pass through the conditions for constructive and destructive interference, and a sinusoidal curve results.

The interferometer is needed in order to convey to the detector which wavelengths of light are present in the signal, and at what amplitudes. It does this by producing a periodically varying signal for each wavelength present in the incident light, as in equation 1.10. The intensity, I , for a given wavenumber, $\tilde{\nu}$, depends on the path difference between the two arms, x . [10]

$$I(x) = I_0 \{1 + \cos(2\pi\tilde{\nu}x)\} \quad (1.10)$$

The resulting oscillating signal containing all wavelengths is called an interferogram, representing the sum of all the periodic waves contained in the light. The interferogram has a maximum at the point representing a zero-length path difference between the two arms of the spectrometer. Given that each wavelength was encoded by the interferometer before passing through the sample, the interferogram can be converted into a power spectrum, S , by applying the Fourier integral:

$$S(\tilde{\nu}) = \int_{-\infty}^{\infty} I(x) \cos(2\pi\tilde{\nu}x) dx \quad (1.11)$$

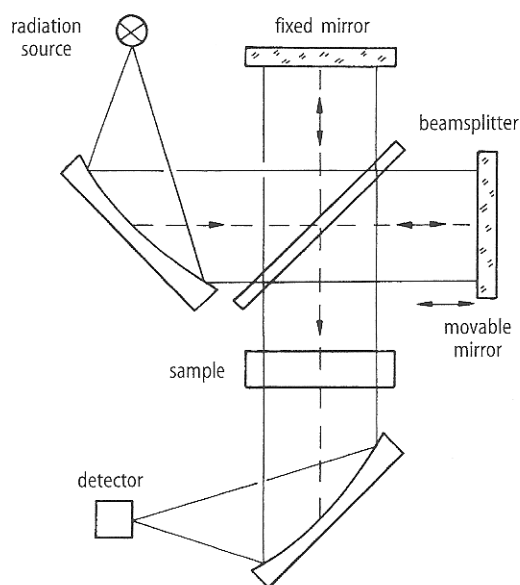


Figure 1.10: **Typical Fourier Transform Spectrometer.** Simplified view of a typical Fourier Transform spectrometer including a Michelson interferometer. The mirror on the right is moved at constant velocity to obtain a periodically varying signal for each wavelength of incident light. [10]

The main advantages of FTIR over the grating spectrometer are the multiplex (or Fellgett) advantage and the throughput (or Jacquinot) advantage. The multiplex advantage occurs because all wavelengths of light are collected at once during Fourier transform spectroscopy. Since the wavelengths of light must be measured sequentially when using a grating, the FT technique can drastically reduce scan times to collect spectra. This allows many hundreds or thousands of scans to be collected in a reasonable amount of time, and then averaged to improve the signal-to-noise ratio.

The throughput advantage occurs because all of the light emitted by the lamp can be used to produce a spectrum when doing Fourier transform spectroscopy. When using a grating spectrometer the first maximum in the interference pattern produced by the grating at a particular wavelength would be applied to the sample. The rest of the light at that wavelength would be wasted. Since no such limitation is necessary, much more light at a particular wavelength is applied to the sample when doing FT spectroscopy. This is especially important with samples like the ones used in this project, since the broad water absorptions present make any light passing through the sample valuable.

1.3 Expected Results

Infrared spectroscopy has been successfully used to study PS I, and the first step of this project was to attempt to duplicate some of those results. Notable authors in this field include Gary Hastings[12, 13], Jacques Breton[3, 4], and Bridgette Barry[2]. FTIR is used to study PS I because it is particularly sensitive to the substance being studied. As noted by Hastings, FTIR has “molecular specificity.” Given that this is the case, changes should be visible in the spectrum when a PS I sample is exposed to light, and they should be reproducible.

The region of interest for the light-dark PS I difference spectra obtained by Hastings and Breton

is approximately $1800\text{-}1200\text{ cm}^{-1}$. In this region, significant differences were seen between the light and dark spectra, which are the IR spectra collected when the PS I samples were illuminated or not illuminated by a source of visible light, respectively. The $1800\text{-}1200\text{ cm}^{-1}$ spectral region is also useful because the water absorptions are not as severe as at higher wavenumbers. Where water absorptions in the spectrum are high, barely any infrared light passes through the sample, and data quality becomes suspect.

The desired light-dark signal comes in part from the stretching mode of the carbonyl group of the phylloquinone in PS I, shown in Figure 1.7. The carbonyl stretching mode is a strong absorption that occurs in the region of $1630\text{-}1780\text{ cm}^{-1}$, depending on the local bonding environment.[19] Chlorophyll, however, also contains carbonyl groups, as shown in Figure 1.5. Only four bonds per PS I particle form the desired light-dark signal, since there are two phylloquinone molecules with two carbonyl bonds each. There are three carbonyl bonds in chlorophyll, and many thousands of chlorophyll molecules per PS I particle.

The consequence of the abundant chlorophyll is that the signal distinguishing the chlorophyll carbonyl from the phylloquinone one, shown in Figure 1.11, is very small by comparison. The two carbonyl modes are distinguished since phylloquinone is more likely to be reduced during the light spectra than during the dark, whereas the chlorophyll signal should be unchanged.

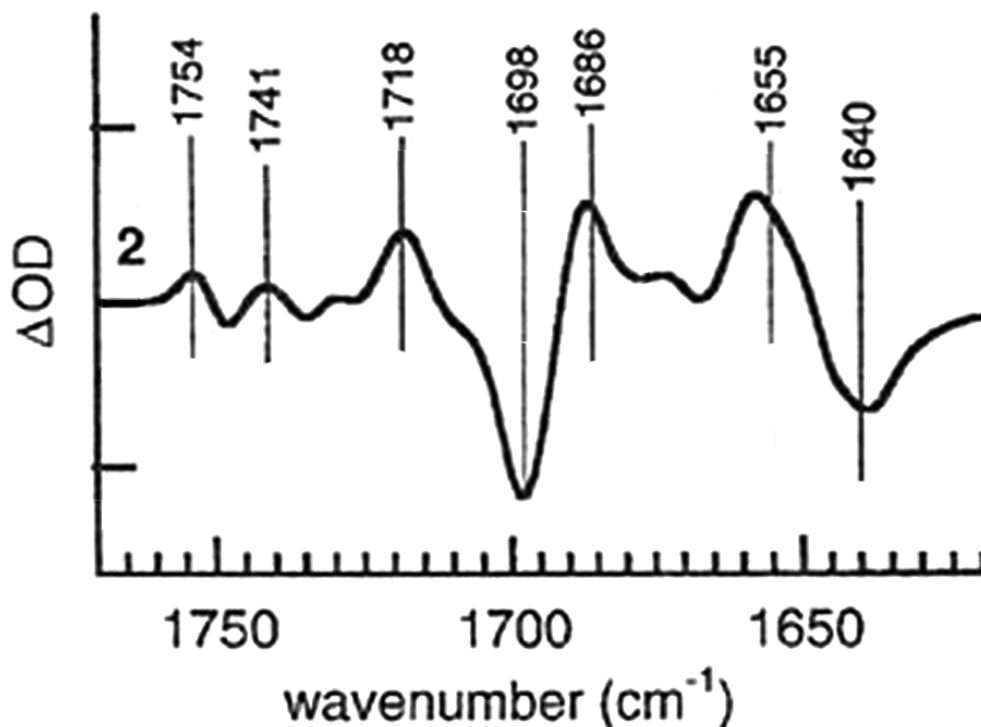


Figure 1.11: **Hastings' PS I Light-Dark Absorption Difference Spectrum.** The first goal of this project was to duplicate this spectrum. Hastings gives the units of the distance between tick marks as “an OD change of 2×10^{-3} .” This dimensionless unit probably indicates that the axis label should be Δ Absorbance.[12]

For comparison, a spectrum obtained by Breton is shown in figure 1.12. The same band shifts are evident, especially at 1697 cm^{-1} , 1637 cm^{-1} , and 1656 cm^{-1} .

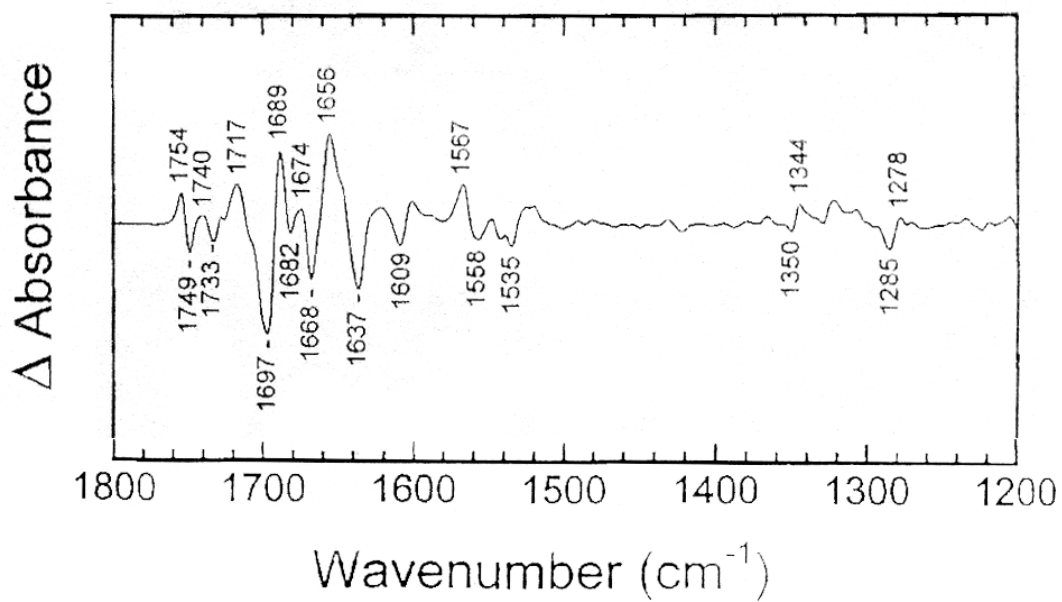


Figure 1.12: **Breton's PS I Light-Dark Absorption Difference Spectrum.** Breton's spectrum shows similar bands to those of Hastings, as well as a low noise level between 1400-1500 cm^{-1} . [3]

Chapter 2

Methods

This section begins with a discussion of the technical details of data production, collection, and presentation. Following that is a discussion of the obstacles encountered during experimentation, and the solutions employed.

2.1 The Light Source and Detector

The spectrometer used was a Bruker IFS 66/V. A globar was used as the spectrometer's light source, meaning the source used to create the spectra, rather than the actinic source used to oxidize P₇₀₀. A globar is an electrically heated rod that emits mid-infrared light. The rod is typically heated to approximately 1150K, and may emit in the broad region from 50-7500 cm⁻¹, although the spectra taken in this lab did not approach those limits.[7]

A Potassium Bromide (KBr) beamsplitter was used. Although it must be stored carefully, this material works well for mid-infrared data collection since it has no absorptions in the region.

A photoconductive MCT (mercury cadmium telluride) detector was used in these experiments. The model was FTIR-24-1.0, made by Infrared Associates, Inc. The conductivity of the photoconductor increases when light of energy greater than the band-gap of the material strikes it. As light strikes the semiconducting material, an electron is promoted to the conduction band and the resistance of the material decreases.[1]

The MCT was cooled by liquid nitrogen to reduce the number of thermally produced conduction electrons, thus increasing the change in resistance produced by absorbed photons. It was also evacuated to thermally isolate the cooled detector and to prevent absorptions by air in the detector itself. The MCT is small and easy to work with, and has a reasonably fast response time.

2.2 Photosystem I Samples

The cyanobacteria *Synechocystis* 6803 is widely used in the study of PS I, since it produces a relatively large amount of the complex. The PS I particles used for experimentation in this project were generously provided by Dr. Art van der Est. The samples came in the form of an aqueous, green material containing chlorophyll and PS I particles. The light capturing apparatus surrounding the PS I reaction centre, consisting of many chlorophyll molecules, was intact in the samples. No electron donors or acceptors were added to the solution.

Two types of samples were used, and were prepared as follows; first, a wild type cyanobacteria (probably *Synechocystis* 6803) was passed through a French press, which is essentially a chamber with a piston and a very small valve. When the cells were made to pass through the valve they experienced a high shear stress that tore them apart.

A centrifuge at low speed was used on the resulting cell particles, so that the soluble material and large particles could be removed. PS II has a very different molecular weight from PS I, so it was removed as well. At this point the sample preparations of the two types differed.

For the type 1 samples, a detergent was added to make the membrane soluble. For the type 2 samples, a centrifuge was carefully prepared with layers of sucrose solution. This created a density gradient, and the type 2 sample was applied to the top, where the density was lowest. When the mixture was spun in the centrifuge at high speed, bands of known density appeared and the band containing the PS I particles was selected. The chlorophyll concentrations shown in Table 2.1 were estimated by one of Dr. van der Est's graduate students.

Sample	Preparation	Chlorophyll Concentration
Type 1	Detergent	2.6 mg/ml
Type 2	Sucrose gradient	1.4 mg/ml

Table 2.1: **Approximate Chlorophyll Concentration of Prepared Samples.** The type 2 samples were of higher quality, since there was less chlorophyll to interfere with the desired signal.

The type 2 samples were considered to be of higher quality since the chlorophyll concentration was lower. This factor is important because the chlorophyll molecules have an absorption in the same area as the desired signal on the light-dark difference spectra, as described in Section 1.3.

2.3 Generation of the Spectra

Data was collected from the spectrometer using Bruker's OPUS software. OPUS was used to compute the ratios of the sample and reference spectra, and then convert the data to absorbance type rather than transmission. Data was then exported in the *Data Point Table* format.

The Physica scripting and plotting software was used to compute the difference spectra, if necessary, and then draw a smooth curve through the data. The curves were drawn using the Physica `interp` command. This command causes the curves to pass through the original data points, and the intervening areas are filled using cubic splines under tension.[5] Generally a vector of 6000 points was generated between 500 and 3500 wavenumbers, with the tension set to 25. The tension determines the shape of the resulting fit, with a higher tension producing sharper peaks.

2.4 Problems and Solutions

The majority of the time spent on this project consisted of designing and assembling the experimental apparatus so that the photosystem samples could be studied using the spectrometer. Many design challenges were encountered that needed solving. This section will discuss the problems and explain the implemented solutions. The problems discussed will be:

1. Water Absorption
2. Sample Holder Material
3. Air Absorptions
4. Actinic Light Source Intensity
5. Signal Variance
6. Signal Averaging

2.4.1 Water Absorption

A major problem to overcome was that the samples were very wet, and water has very strong absorptions in the region of interest. To remove some of the water, the samples were freeze dried. This reduced the water absorptions while concentrating the PS I particles. The most problematic water absorption was the O-H bend mode, since it is typically found at 1643 cm^{-1} . This band is labelled in many of the later figures.

2.4.2 Sample Holder Material

A suitable sample holder was needed to mount the PS I particles in the light path. Hastings and Breton had generally pelleted their PS I samples and squeezed them between CaF_2 windows. As no Calcium Fluoride was readily available, a sample holder material was sought from the materials at hand. It was necessary that the sample holder material would pass both visible light for the actinic (P_{700} oxidizing) light source and IR light in the region of interest (about $1200\text{-}1800\text{ cm}^{-1}$.)

Sample Holder 1: Polypropylene Envelope

Sheets of Polypropylene were available in the lab. Polypropylene passes visible light and was found to have very narrow absorptions in the infrared, as shown in Figure 2.2.

The lines of the spectrum in Figure 2.2 are very sharply defined, and very strong. This is probably because of the large numbers of essentially identical bonds in the polymer molecule, as shown in Figure 2.1. This piece would repeat many times in both directions, forming the long chains typical of polymers.

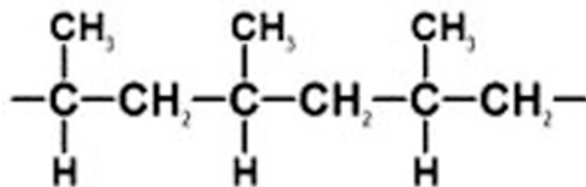


Figure 2.1: **Chemical Structure of Polypropylene.** A piece of a typical polypropylene molecule showing its C-C and C-H bonds. This piece would repeat many times in both directions.

Note that only C-C and C-H bonds exist in polypropylene. C-C bonds lack a dipole moment, and so do not appear in IR spectra. The stretching mode of the C-H bond absorbs strongly in the region $2850\text{-}2950\text{ cm}^{-1}$, as observed in the spectrum. The C-H bending mode absorbs at 1425 cm^{-1} which also corresponds to a strong absorption in the spectrum. The other lines are not easily identifiable, but may be related to dipole interaction between bonds.

Thin film interference is also apparent in the polypropylene spectrum. This manifests itself in the form of the periodic wave across all frequencies, and is especially apparent in the $1500\text{-}2500\text{ cm}^{-1}$ region. Thin film interference occurs in this case because the thickness of the polypropylene is similar to the wavelength of the infrared light. The polypropylene was found to have a thickness of $50 \pm 5\ \mu\text{m}$, while the wavelength equivalent to 2000 cm^{-1} is $5\ \mu\text{m}$.

Thin film interference occurs when the reflected light from the surface of a thin film interferes with the the original light. For a maximum of the interference, the path difference between the reflected and transmitted light, x , must be a multiple of a wavelength difference. The path difference

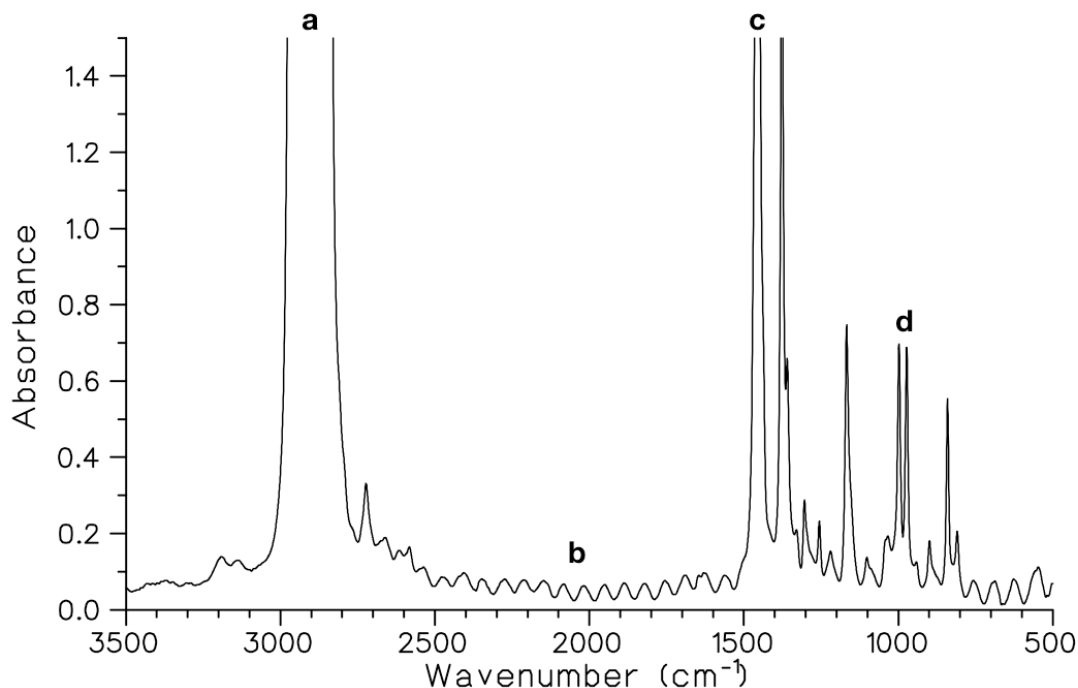


Figure 2.2: **Polypropylene Absorption Spectrum.** Absorption lines are observed in the region of interest, but they are narrow. (a) 2850-2975 cm^{-1} : C-H stretching mode. (b) 1500-2500 cm^{-1} : Thin film interference ripples occur across the spectrum, but are especially apparent here. (c) 1425 cm^{-1} : C-H bending mode. (d) Unknown polypropylene absorptions.

must take into account the index of refraction inside the material, n , which varies with wavelength. The relation is shown in equation 2.1.

$$x = m \frac{\lambda}{n}, \quad m = 0, 1, 2, \dots \quad (2.1)$$

In this case, since the light being examined was transmitted, the interfering light must have been reflected twice within the polypropylene sheet. The path difference would then be twice the thickness of the sheet, t , and the equation 2.1 becomes,

$$\begin{aligned} 2t &= m \frac{\lambda}{n} \\ \lambda &= \frac{2tn}{m}, \quad m = 0, 1, 2, \dots \end{aligned} \quad (2.2)$$

Any wavelength for which this condition is satisfied would have a maximum in the interference pattern, and the sinusoid shown in Figure 2.2 results.

The first attempt at a sample holder was to create an envelope from polypropylene, pour a wet sample into it and mount it vertically in the light path by taping it to an aperture. An example spectrum using this sample holder is shown in Figure 2.3. This technique had several problems.

First, the concentration of chlorophyll in the samples appeared to be very low. Instead of a rich colour, the liquid was barely tinted green. The desired absorption difference signal was expected to be very weak, so a higher concentration of PS I particles in the light path was desired.

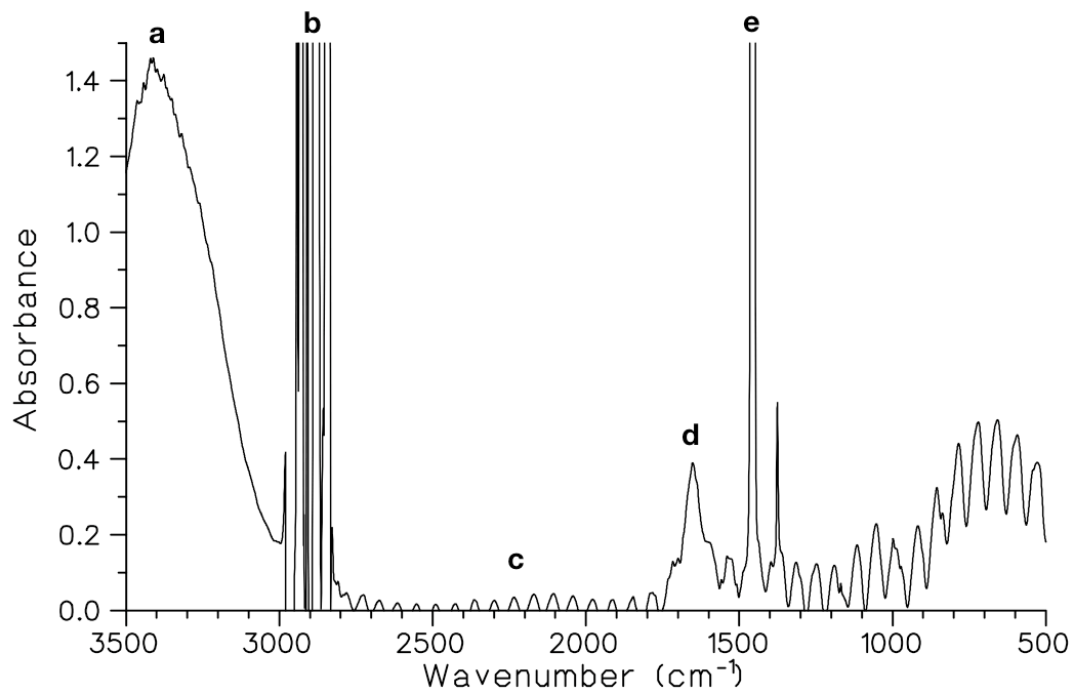


Figure 2.3: **PS I in Polypropylene Envelope Absorption Spectrum.** The water absorptions and thin film interference lines are significant. (a) 3400 cm⁻¹: O-H symmetrical and asymmetrical stretching mode. (b) 2850-2975 cm⁻¹: This feature occurs because almost no light passes through the polypropylene in this range. (c) Thin film interference fringes appear across the spectrum. (d) 1650 cm⁻¹: This band is probably a combination of the O-H bending mode of water and the C=O stretching mode from the PS I samples. (e) 1425 cm⁻¹: C-H bending mode of polypropylene.

A related problem was the amount of water in the sample. In the region near 3400 cm^{-1} there is such heavy water absorption that practically no light passes through the sample. This absorption is not worrisome because it is outside the region of interest, however the peak at 1643 cm^{-1} occurs in the middle of the desired area. This peak is attributable to the O-H bending mode of liquid water, and an absorption here could drown out the desired light-dark signal.[10, 22]

The polypropylene lines were also somewhat problematic. Although the region of highest interest was $1600\text{-}1775\text{ cm}^{-1}$, in order to compare to Hastings' results, data in the region of $1200\text{-}1600\text{ cm}^{-1}$ was desired as well, in order to compare with Breton's results. The very strong polypropylene absorption at 1460 cm^{-1} would preclude data collection at this frequency if this sample holder were used.

Finally, the thin film absorption lines present in the spectrum were problematic. These lines occur throughout the spectrum and would vary in position if any piece of the experimental apparatus was moved even slightly, meaning that they would not subtract out of the difference spectrum. The size of the interference lines would almost certainly drown out the light-dark signal.

Sample Holder 2: Polypropylene Slide

The next attempt at a sample holder was simply freeze-drying the PS I particles overnight on a rectangular sheet of polypropylene. This caused the sample to become very dry and adhere to the polypropylene sheet, which was taped to an aperture in the light path. An example spectrum using this sample holder is shown in Figure 2.4. Although the absorption peaks appear to be higher in this spectrum than in Figure 2.3, taken with the envelope, note that the absorption level never reaches zero across all frequencies. This is probably due to scattering, since this sample was much more concentrated.

The features are described in the caption of Figure 2.4. There is a new feature near 1050 cm^{-1} that was not in Figure 2.3. This feature probably appeared because the samples were much more concentrated.

This sample mounting technique was problematic for several reasons. First, others have found that when a PS I sample is too dry it does not yield a good light-dark difference spectrum, and this preparation method caused the samples to be very dry. Hastings has suggested that spurious absorptions appear when the proteins of PS I are dehydrated. Discussing the inconsistent difference spectra (DS) among several researchers, he says, "The use of dehydrated samples could possibly explain why the (P700⁺-P700) FTIR DS reported by Kim et al. do not closely resemble previously published (P700⁺-P700) FTIR DS..."[14]

The second problem with this mounting technique was that the polypropylene caused thin film interference lines to appear throughout the spectra. These lines were very problematic, as they introduced a large oscillation into the spectra that could mask the features of interest.

Sample Holder 3: KBr Windows

Next, KBr plates were investigated. The KBr plates were placed in the light path inside the spectrometer by using a metal part designed for the purpose, on loan from the chemistry department. The metal apparatus basically consisted of two rectangular pieces with square holes in the middle, screwed together to sandwich the KBr plates.

This material was found to be a suitable alternative, at least optically. KBr passes visible light and has no absorptions in the IR. Figure 2.5 shows a clean spectrum for the KBr plates. Although there is scattering or a broad absorption at higher wavenumbers, none of the deep absorptions seen with the polypropylene are present, and most importantly the thin film interference lines are

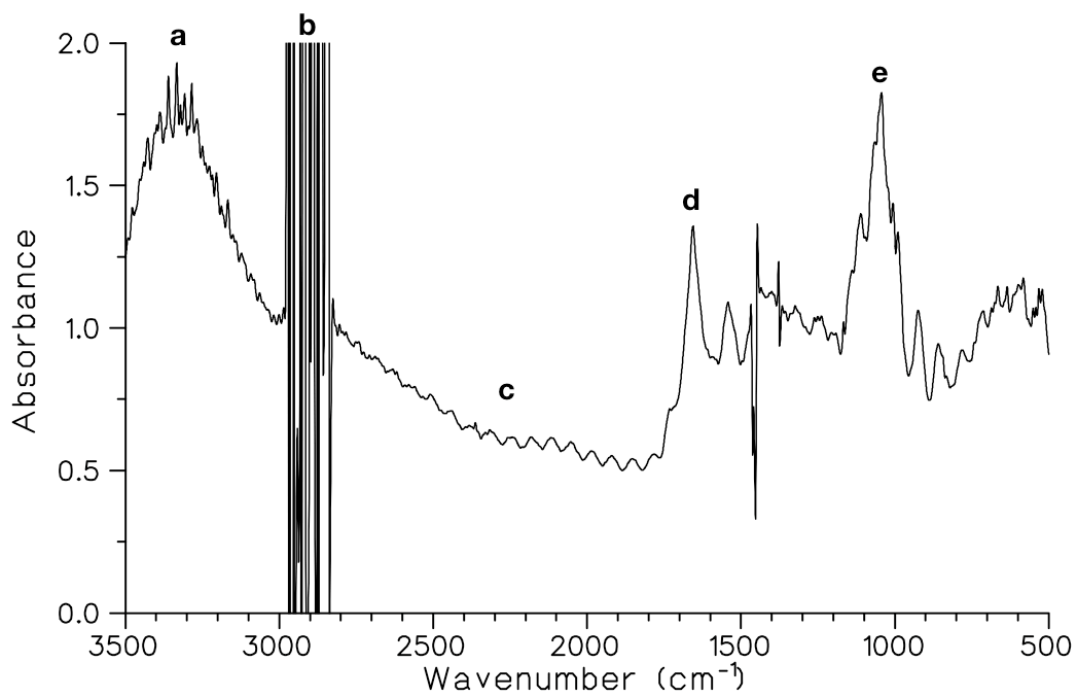


Figure 2.4: **PS I on Polypropylene Slide Absorption Spectrum.** Thin film interference lines are present as a result of the polypropylene thickness being comparable to the wavelength of incident light. **(a)** 3400 cm^{-1} : O-H symmetrical and asymmetrical stretching mode. **(b)** 2850-2975 cm^{-1} : This feature occurs because almost no light passes through the polypropylene in this range. **(c)** Thin film interference fringes appear across the spectrum. **(d)** 1650 cm^{-1} : This band is probably a combination of the O-H bending mode of water and the C=O stretching mode from the PS I samples. **(e)** 1050 cm^{-1} : This band is hard to classify, but may be C-N stretching.[19]

absent. The broad absorption may be due to the hygroscopic nature of KBr, meaning that it tends to absorb water from the air. Because the plates were old and had been exposed to air, they were very cloudy and may have been scattering some IR light.

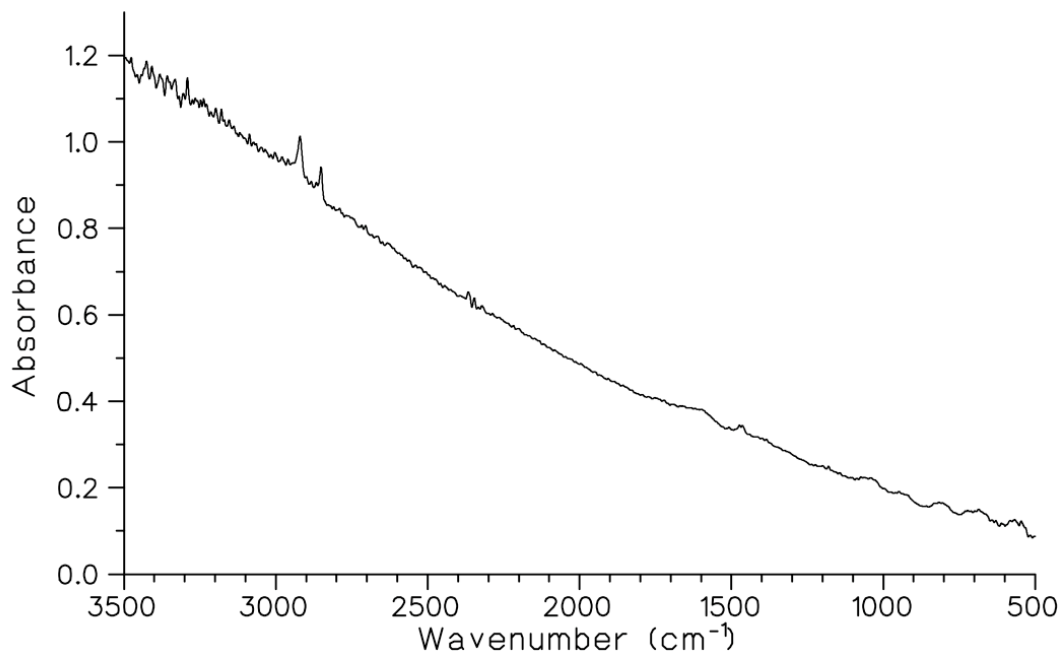


Figure 2.5: **KBr Absorption Spectrum.** Although a broad scattering or absorption is present at higher wavenumbers, no sharp absorption lines are observed in the region of interest, and no thin film interference is present.

The data on KBr provided by a manufacturer confirms that it has no absorptions in the region of interest. Figure 2.6, provided by the manufacturer, shows KBr transmitting 90% of incident light between about 50000-333 cm^{-1} .

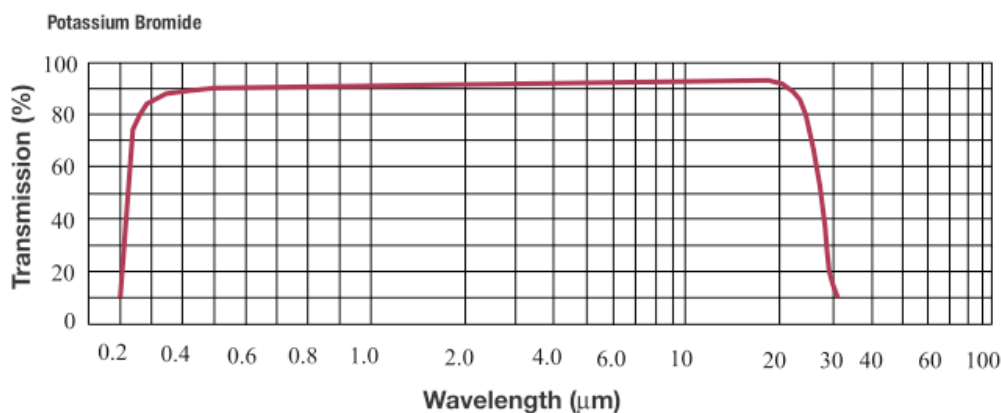


Figure 2.6: **Optical Properties of KBr.** The manufacturer's data shows that Potassium Bromide transmits light in the visible and infrared ranges down to about 333 cm^{-1} . [20]

A spectrum was produced using a partially freeze-dried sample between KBr plates, and is shown in Figure 2.7. Comparing this spectrum with Figure 2.4 using polypropylene is very instructive. The KBr spectrum is much cleaner since it has none of the thin film interference lines. It also has

very strong water absorptions, but the amount of water in the samples can be controlled using the freeze drying time.

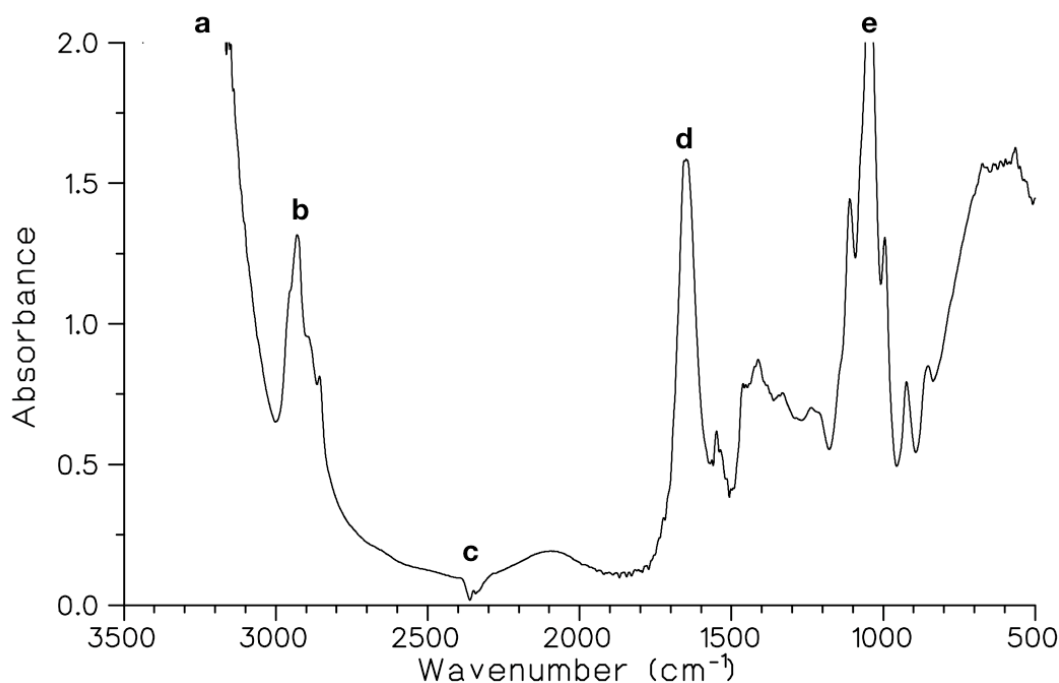


Figure 2.7: **PS I in KBr Sample Holder Absorption Spectrum.** A spectrum of a PS I sample between KBr windows, with KBr as a reference. Strong water absorptions are visible, but none of the thin film interference lines are present. (a) 3400 cm^{-1} : O-H symmetrical and asymmetrical stretching mode. (b) 2950 cm^{-1} : Probably a C-H stretching band, although now unrelated to polypropylene. (c) This feature is due to CO_2 , described in Section 2.4.3. (d) 1650 cm^{-1} : This band is probably a combination of the O-H bending mode of water and the C=O stretching mode from the PS I samples. (e) 1050 cm^{-1} : This band is hard to classify, but may be C-N stretching.[19]

The KBr sample holder was an improvement over polypropylene. KBr is very hygroscopic, however, and is quite fragile. The hygroscopic nature of KBr was problematic because the samples, though partially freeze-dried, still contained a lot of water. The KBr plates used became slightly pitted after being in contact with PS I samples for an extended period of time, and would no doubt have exhibited more damage and cloudiness, since the light-dark spectra require that the sample be left in its holder for many hours while data is collected.

The KBr was also quite soft. While mounting one sample into the metal apparatus, one of the KBr slides cracked and had to be replaced. The plates were also cloudy from age and having been left out of a desiccator. This seemed likely to increase scattering and reduce the useful light passing through the PS I samples.

Sample Holder 4: CaF_2 Windows

A material was needed that was fairly hard, had the optical properties of KBr, but was not hygroscopic. According data supplied by a manufacturer, CaF_2 was found to fit these criteria. The optical properties, as given by the manufacturer, are shown in Figure 2.8. The substance is seen to transmit above 90% of incident light over a broad region. The limits of the region are $0.1\mu\text{m} = 100\text{ nm}$, in the

ultraviolet spectrum, and $10\mu\text{m} = 1000\text{ cm}^{-1}$, in the infrared. The documentation also described the plates as relatively hard.

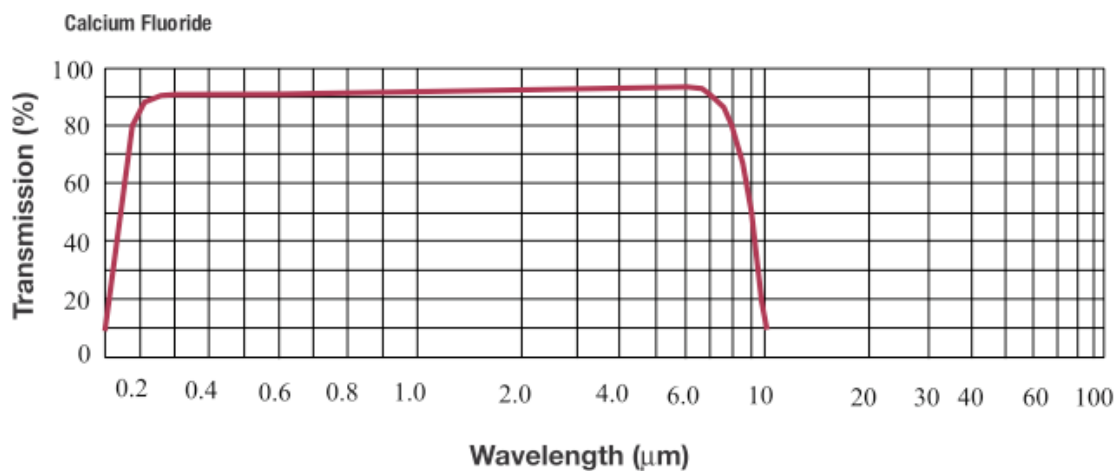


Figure 2.8: **Optical Properties of CaF_2 .** This information was provided by a manufacturer of CaF_2 windows. Calcium fluoride is seen to transmit light in the visible and infrared ranges down to about 1000 cm^{-1} . [20]

An absorbance spectrum was taken for the obtained CaF_2 windows, and is presented in Figure 2.9. The spectrum is acceptable since there are no strong absorptions in the region of interest. All light is absorbed below 1000 cm^{-1} , but this is not problematic for the PS I spectra. The small bump at 1750 cm^{-1} and the overall absorbance across the spectrum being higher than the manufacturers specifications may be due to variance in the light level, since there was a period of days between the time that the reference and sample spectra were taken for this plot.

2.4.3 Air Absorptions

Since it was necessary to hit the samples with an actinic (P_{700} oxidizing) light source for some of the spectra, the early spectra were taken with the spectrometer uncovered and open to the air. This caused lines to appear in the spectra due to the atmospheric gases. If the lines had been static, they would have been cancelled when sample-to-reference ratio was calculated. The absorption levels caused by the air were changing with time, however, and problematic bands appeared in the absorbance spectra.

The absorbance spectrum presented in Figure 2.10 shows the atmospheric absorptions in sharp relief. This absorption spectrum was taken using air as the sample and an evacuated spectrometer as the reference. The worst bands were the jagged peaks that appeared across the region of interest from $1300\text{--}2000\text{ cm}^{-1}$. These lines can be attributed to atmospheric water. Absorption features also appeared near 2350 cm^{-1} and 675 cm^{-1} . These bands are attributable to the asymmetric stretching and bending modes of CO_2 , respectively. [10, 16]

The problem of air absorptions could have been solved by sealing the spectrometer with the sample inside. Hastings took his spectra this way, with static air absorptions present that disappeared when transmission spectra were calculated. However the spectrometer being used for this project had no access for visible light to enter. This was a necessary feature for gathering a light-dark difference spectrum. It was decided that the best way to solve the problem was to evacuate the spectrometer and put the sample in a separate chamber.

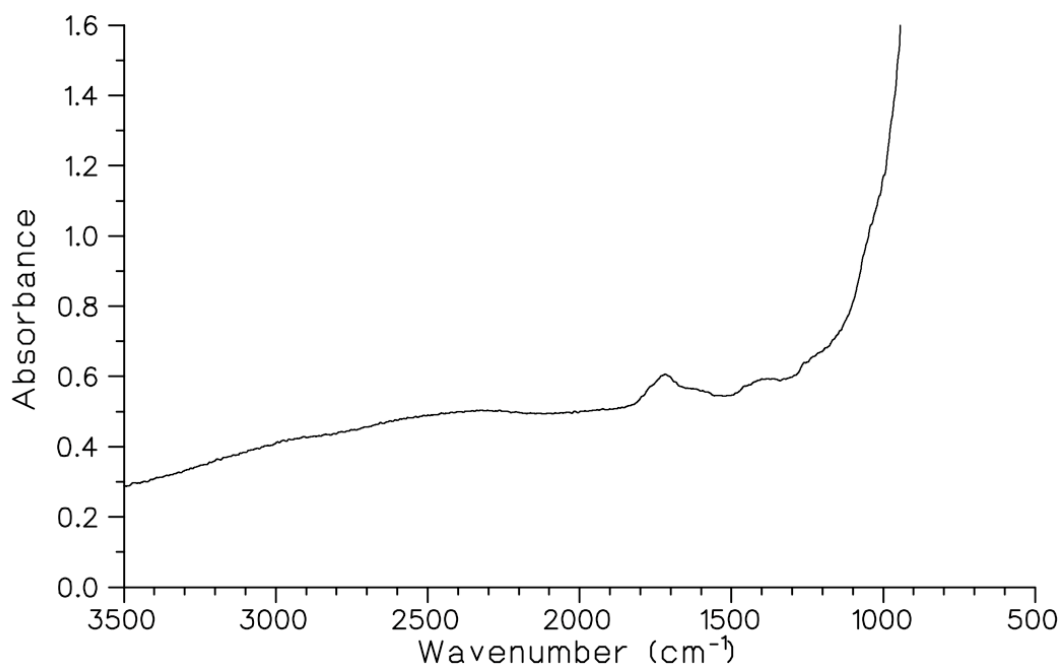


Figure 2.9: **CaF₂ Absorption Spectrum.** The spectrum is remarkably clean compared to earlier materials. CaF₂ absorbs all light below 1000 cm⁻¹, but that was not problematic for this project. The feature seen near 1700 cm⁻¹ most likely occurred because of variation in the source intensity, due to the long time between taking the sample and reference spectra to produce this plot.

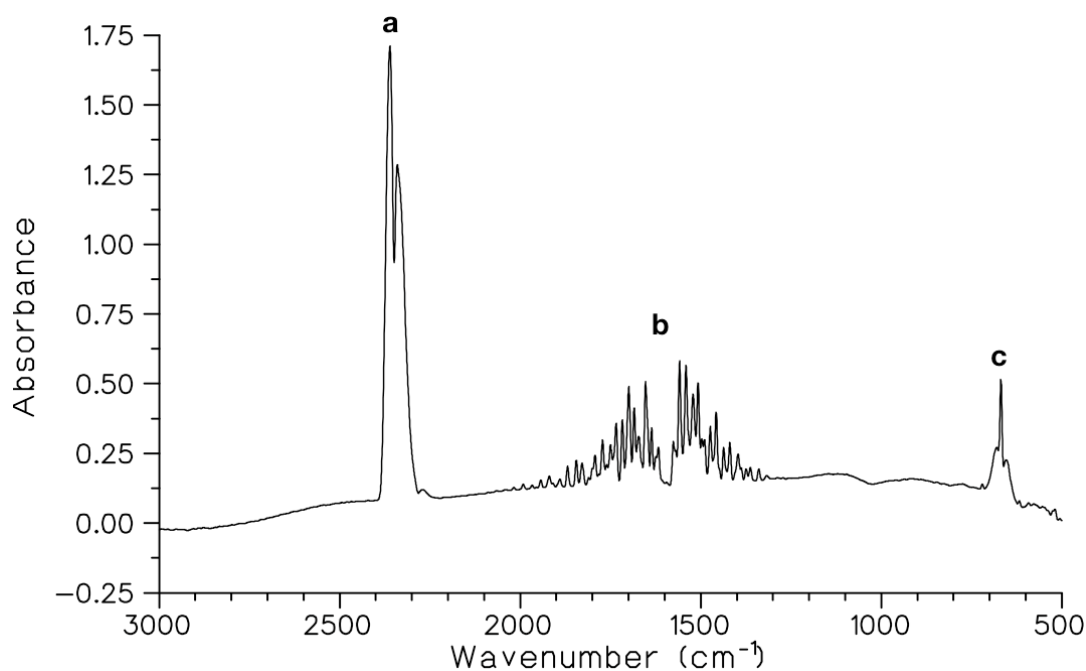


Figure 2.10: **Laboratory Air Absorption Spectrum.** A spectrum of air, with the Bruker evacuated to 5 millibars as the reference. (a) 2345 cm⁻¹: CO₂ asymmetric stretching mode. (b) 1300-2000 cm⁻¹: Atmospheric H₂O (steam) (c) 667 cm⁻¹: CO₂ bending mode.

The chamber holding the sample could not be evacuated, however, since the sample was volatile. To eliminate the air absorptions from this section of the light path, nitrogen gas was pumped through the chamber with positive pressure to expel any air. N₂ gas, being a symmetric molecule, does not have any absorptions in the infrared.

2.4.4 Actinic Light Source Intensity

An important consideration when trying to produce the light-dark difference spectra was whether the actinic light source (the source meant to oxidize P₇₀₀) was intense enough. The actinic light source needed to be intense enough to produce a charge separation in enough of the PS I particles that the signal could be detected. Throughout the process of experimenting with sample holder materials and taking spectra, the actinic light source was also varied. The ideal source would be intensely focused on the sample, and produce light at a wavelength that corresponds to a strong absorption for PS I.

While the spectra were being taken in air, access to the sample was easy and an incandescent source was originally used. It had an aluminum reflector that helped direct light onto the sample. Later a halogen lamp was used. The light source was on the end of a long, flexible neck of the lamp, so it could be positioned within a few centimetres of the sample. The source seemed intense compared to the incandescent bulb, but still light-dark difference spectra were not being produced. The possibility that the actinic source was not intense enough could not be ruled out.

When the sample was placed in the nitrogen environment, light access to the sample was only possible through a small glass window. A laser was the ideal choice in this case, producing an intense light beam that could be directed onto the sample. Hastings had used a 5 mW helium neon (He-Ne) laser as the actinic light source for his static FTIR measurements.[12] A 4 mW red He-Ne laser was available within the department, and was used for this purpose. A diverging lens with focal length $f = -144$ mm was placed in the path of the laser to produce a larger spot size on the sample, as shown in figure 2.12.

2.4.5 Signal Variance

As the spectra were collected, it was evident that the signal level was not constant even though there was no longer any air in the light path. The change in absorbance over most of the spectrum was visible even through reasonably short scan times. The time varying signal was mainly due to the fact that the PS I samples were not securely held in place between the CaF₂ windows.

The procedure for mounting the samples after they were freeze dried was that the sample would be very lightly sandwiched between two CaF₂ windows, which were then placed in the sample holder. The sample holder applied light pressure to the windows, but only just enough to keep the windows in place. When too much pressure was applied, the PS I sample simply squeezed out and was wasted, leaving a very thin solution behind.

This meant that without much holding it in place, the PS I sample slowly ran down the windows and thickened at the bottom over time. Since the spectrometer light was passing through the sample near the middle, the amount of absorbance and scattering observed decreased over time, as the amount of sample in this area decreased. This phenomenon is shown in Figure 2.11. The broad absorbance peak is due to the O-H bending mode of water, which occurs at 1643 cm⁻¹. [22] The signal variance was problematic because absorptions like the one shown in Figure 2.11 mask the desired light-dark signal.

The solution to the problem was to make a spacer to be placed between the CaF₂ windows. The

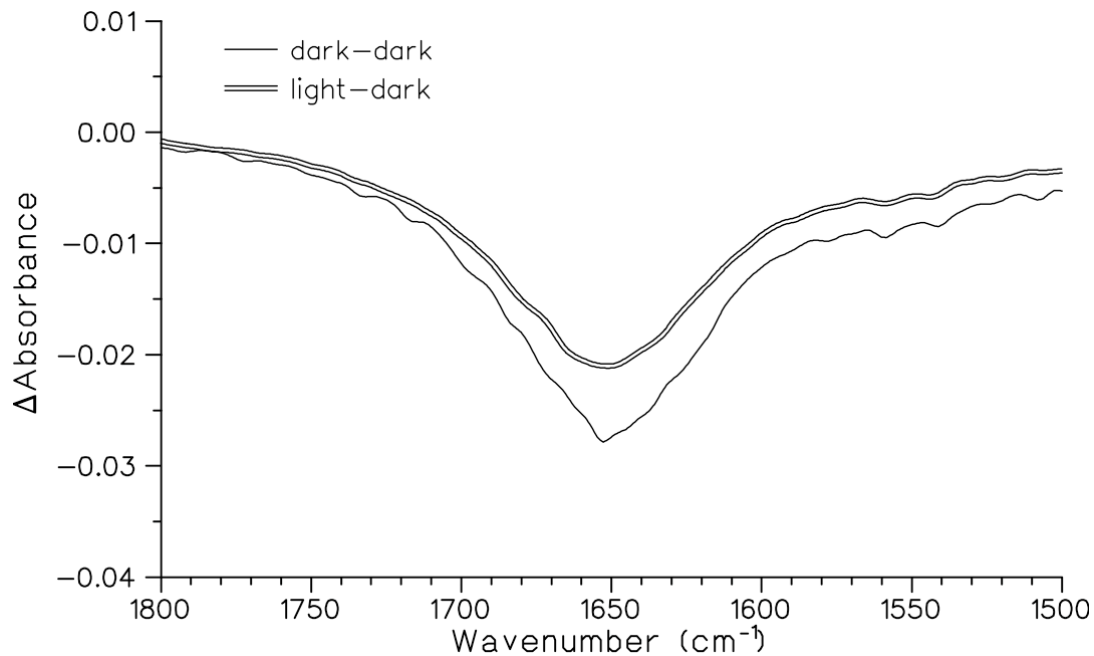


Figure 2.11: **Light-Dark Spectrum Showing Signal Variance.** The signal varied as the spectra were taken because the sample was not stable between the CaF_2 plates. The broad absorption shown is probably the O-H bend mode of water, usually seen at 1643 cm^{-1} , and is directly in the region of interest.

spacer was shaped like a disc with its center removed, and was originally made of polypropylene. The polypropylene proved too thick, however, since not enough light was passing through the samples to produce an acceptable spectrum. The thickness of the polypropylene was measured as $50 \pm 5 \mu\text{m}$. A mylar spacer proved thin enough to provide a good quality spectrum. Its thickness was measured as $20 \pm 5 \mu\text{m}$.

This spacer ring was placed between the CaF_2 windows, and then the sample was added to the middle. This allowed the windows to be pressed together firmly and better held the sample in the centre of the windows. The edges of the windows were then taped to prevent any shifting, and try to counteract any evaporation that may have been affecting the spectra.

2.4.6 Signal Averaging

The desired light-dark signal was very small compared to the background, as explained in section 1.3, so even with the minimization of problematic absorptions in the region of interest, it was necessary to improve the signal-to-noise ratio. The primary way of accomplishing this was to average as many spectra as possible.

This technique takes advantage of the fact that the desired signal should be constant, whereas the noise portion of the measured signal should be irregular. The idea is that by taking the same measurement repeatedly and averaging the resultant spectra, the irregular portions should tend to cancel out, while the desired signal remains. The standard deviation of N measurements should be smaller than the standard deviation of a single measurement by a factor of \sqrt{N} . In practice it can be approximated that N measurements improves the signal-to-noise ratio of a single one by a factor of \sqrt{N} . [8]

Specifically, the chlorophyll absorptions should remain constant through the light or dark spec-

tra, while the phylloquinone absorptions should change slightly. By taking many thousands of scans, the change should be visible above the noise. The first light-dark spectra in this project were taken with 1000 scans, and this was gradually increased to 30000 scans in the final spectrum. This came at the expense of measuring time, of course, as the final spectrum took 14 hours of scanning to complete.

2.4.7 Final Sample Holder

The final sample holder, shown in Figure 2.12, incorporated all of the solutions discussed thus far, including a flowing nitrogen environment, mounted CaF_2 plates and window access for the laser light. The depth was also designed so that the light exiting the spectrometer would be focused on the detector.

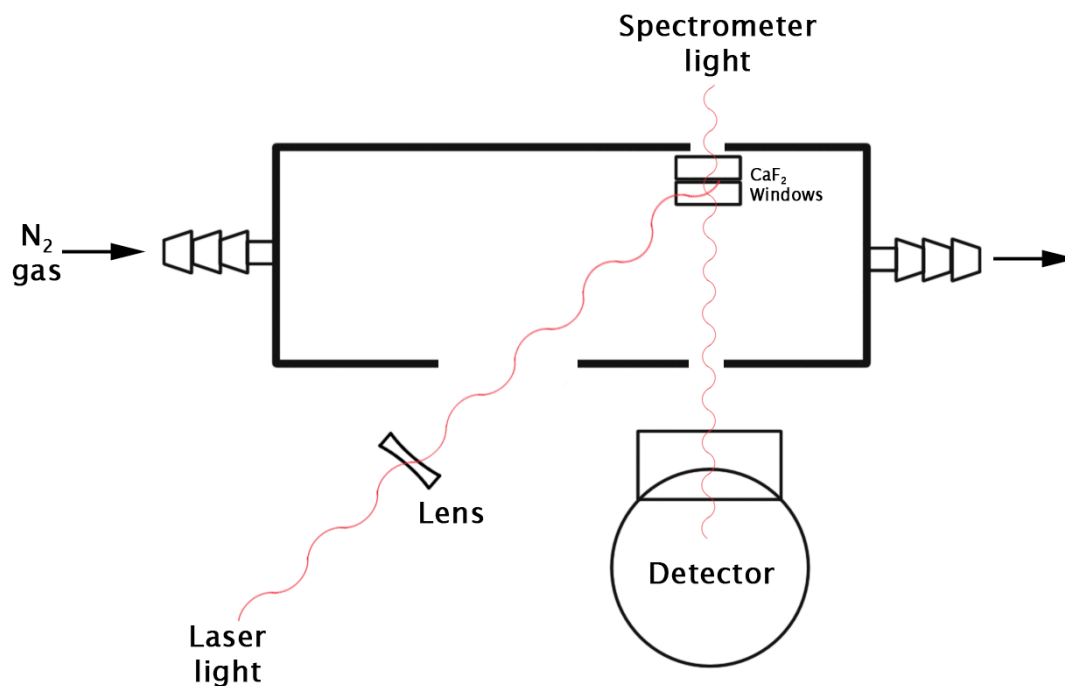


Figure 2.12: **Final Experimental Apparatus.** A representation of the apparatus finally used to study the PS I samples included mounts for the CaF_2 windows and the detector, a flowing nitrogen environment, and laser light access to the sample.

Chapter 3

Light-Dark Difference Spectra

Many light-dark absorbance difference spectra were obtained, although none definitively showed the desired signal around 1700 cm^{-1} . This section will examine three of the light-dark difference spectra obtained.

3.1 Polypropylene Slide Sample Holder

The light-dark difference spectrum shown in Figure 3.1 was obtained using the polypropylene slide as a sample holder with a PS I sample freeze dried onto it, described in Section 2.4.2. The spectrum was obtained using 2500 scans, with a resolution of 5 cm^{-1} .

At first this spectrum may seem to show several bands, but what appears is probably noise. Some of the bands may be caused by thin film interference, since this sample holder suffered heavily from that problem. A comparison with Hastings' spectrum from the same region, shown in Figure 1.11, reveals that this spectrum is lacking the expected large bands at 1698 cm^{-1} and 1686 cm^{-1} .

A major problem with this spectrum, which was collected early in the project, is that a dark-dark spectrum was not obtained at the same time. Without a dark-dark spectrum for comparison, the noise level in the light-dark spectrum cannot be characterized. For this reason, the results shown are not useful.

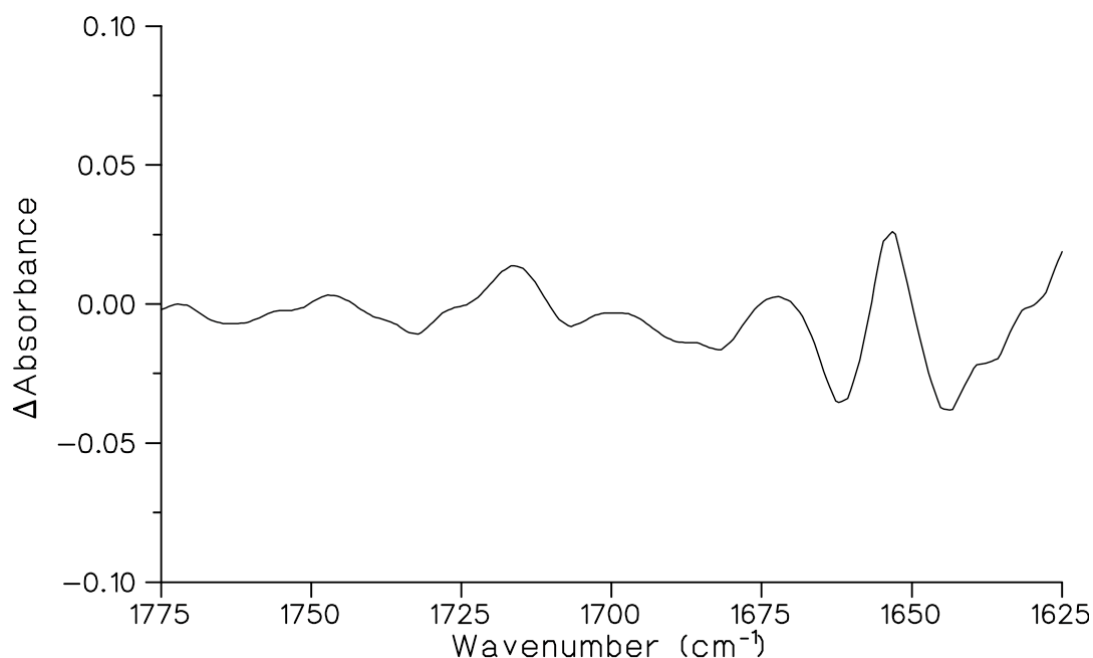


Figure 3.1: **PS I on Polypropylene Slide Light-Dark Difference Spectrum.** An absorption difference spectrum was attempted using 2500 scan light and dark spectra of the PS I particles freeze dried to a polypropylene slide.

3.2 CaF₂ Sample Holder Without Spacer

Two light-dark difference spectra were obtained using the full CaF₂ sample holder apparatus, including the flowing nitrogen, described in Section 2.4.7, but lacking the spacer between the CaF₂ windows.

The spectra, presented in Figure 3.2, were obtained using sample type 1 that had been freeze dried for approximately thirty minutes. 1000 scans for each spectrum were performed, and the spectrometer was set to a resolution of 5 cm⁻¹. Six absorbance spectra were obtained, and subtracted as shown to produce the difference spectra.

Compared to the spectrum of Figure 3.1, the bands are much smaller, further reinforcing the notion that the bands of the previous figure may be due to thin film interference. As in the previous spectrum, the deep bands at 1698 cm⁻¹ and 1686 cm⁻¹, shown in Hastings' spectrum of Figure 1.11, are not present.

Since the dark-dark spectrum is present, the noise level can be characterized. The dark-dark spectrum has ripples on the same order of magnitude as the light-dark spectra. This means that the apparent bands in the light-dark spectra cannot be considered absorbance bands, they must be considered noise.

The change in height observed in the spectrum labelled light2-dark4 is typical of the change in signal that occurred over time before a spacer was introduced, as explained in Section 2.4.5. The shift is due to the changing amount of the sample present in the light path.

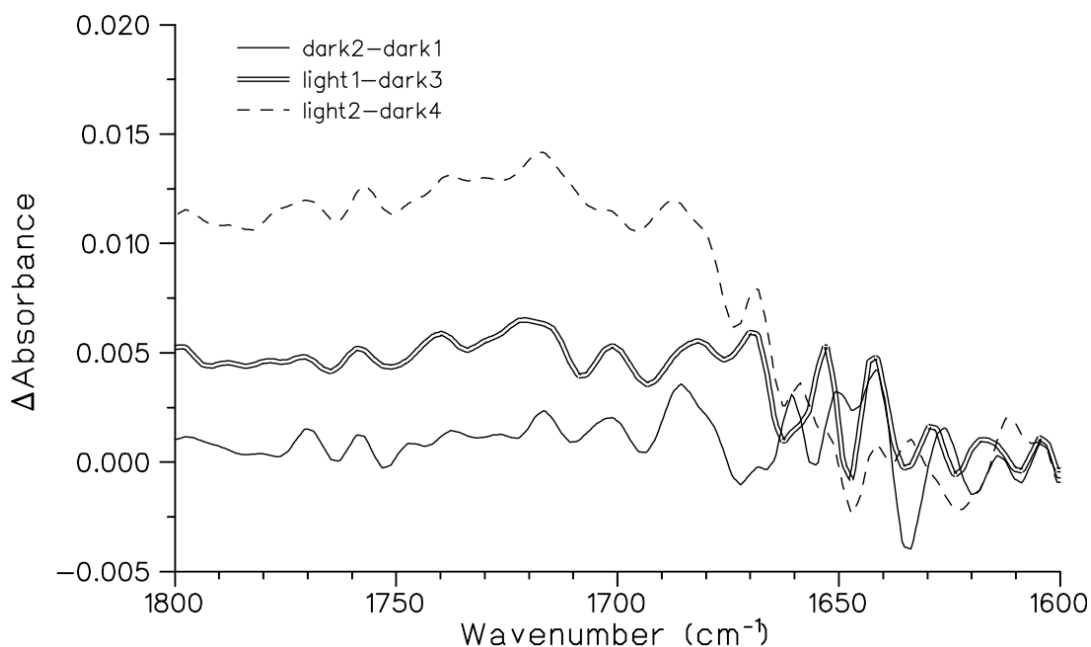


Figure 3.2: **1000 Scan PS I Light-Dark Difference Spectra.** Sample type 1 was used (described in Section 2.2). The dark-dark level is included for reference, and shows that the apparent absorption lines are all on the order of the noise. The heights of the spectra vary due to the changing amount of material present, since a spacer was not used.

3.3 Final Sample Holder

Finally, 30000 scan light-dark spectra were obtained, using sample type 2, and the spectrometer set to a resolution of 5 cm^{-1} . Two dark spectra were obtained along with one light spectrum, using the 4 mW He-Ne laser. To reduce the noise level, thirty thousand scans were obtained for each spectrum in the order shown in Table 3.1.

The spectra were collected in a staggered order to reduce the effects of the variable signal, although those effects were greatly reduced by adding the spacer. Ideally reference spectra would have been gathered along with the light and dark to account for changes in the light source intensity, however this would have extended the total data collection time and required the removal of the sample from its holder. A similar way to deal with the problem of varying intensity would be to take 30000 separate spectra for each of the dark1, dark2 and light results. This would require an electronic and software solution, however, since collecting the data by hand would take a prohibitively long time. The comparatively few spectra collected in this project, with 3 distinct runs of 10000 scans for each case, is a weakness of the technique.

Spectrum	Time Started	Scans Performed
Dark1	15:58	10000
Dark2	17:35	10000
Light	19:15	10000
Dark2	21:15	10000
Light	22:56	10000
Dark1	00:35	10000
Light	02:36	10000
Dark1	04:16	10000
Dark2	05:54	10000

Table 3.1: **Order of Gathered Spectra** The spectra were collected in a staggered order to reduce the effects of the variable signal.

The resultant spectra after 30000 scans were more interesting than previous runs, and are presented in Figure 3.3. The most obvious feature is the large band pointing up in the light-dark2 spectrum and down in the dark2-dark1 spectrum. This is the result of changing water levels over the course of the scanning, since this band is the 1643 cm^{-1} O-H bend mode discussed earlier. A power spectrum showing how little light was getting through at 1643 cm^{-1} is presented in Figure 3.4.

The terrible result for the dark-dark spectrum meant that the data was not trustworthy. The light-dark1 spectrum was interesting, however, because some of the lines appeared close to those obtained by Hastings. A closer view the light-dark1 spectrum in the same region is presented in Figure 3.5. The figure shows a band pointing down at 1699 cm^{-1} , and another at 1670 cm^{-1} . There is a sharp band pointing up at 1660 cm^{-1} . The apparent 1699 cm^{-1} band is also present in the light-dark2 spectrum. These bands are similar to bands in Hastings' light-dark spectrum of Figure 4.1, which shows downward bands at 1698 cm^{-1} and 1667 cm^{-1} , and an upward band at 1655 cm^{-1} .

A further useful comparison can be performed with Breton's light-dark difference spectrum shown in Figure 1.12. The data viewed to 1200 cm^{-1} is presented in Figure 3.6. The noise bands in the obtained dark-dark spectrum at lower wavenumbers are much larger than those obtained by Breton. These noise bands are nearly the same magnitude as the interesting light-dark1 bands near 1700 cm^{-1} , so the light-dark bands cannot be trusted.

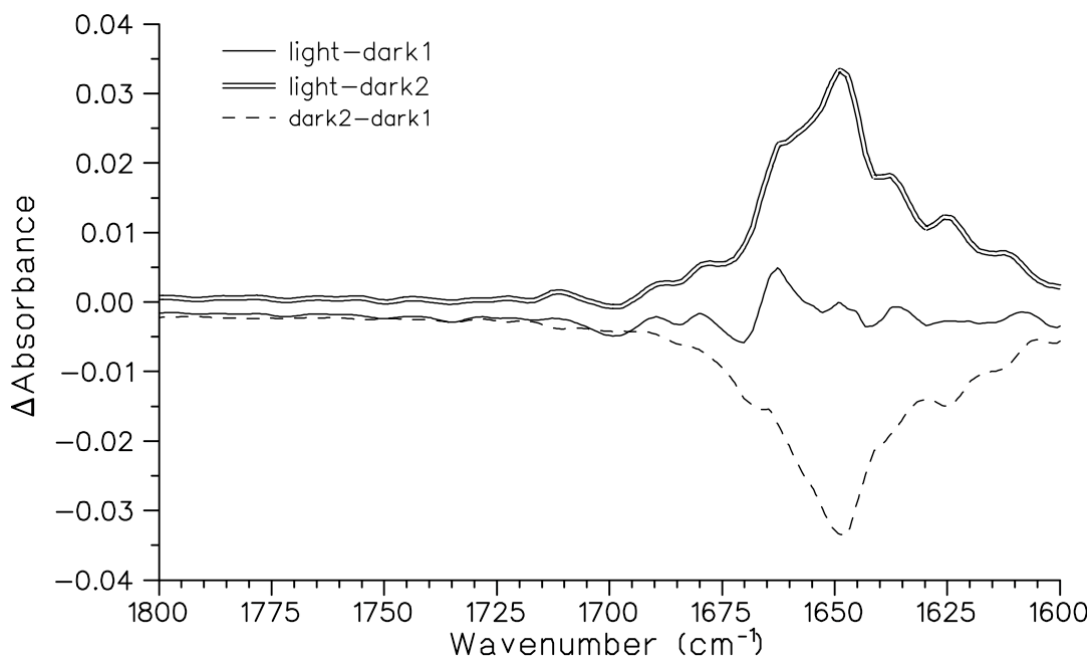


Figure 3.3: **30000 Scan PS I Light-Dark Difference Spectra.** Sample type 2 was used (as explained in Section 2.2). The full sample holder with a spacer between CaF_2 windows and flowing N_2 gas was used. The dark-dark level is included for reference, and shows a broad band at 1643 cm^{-1} corresponding to the O-H bend mode of water.

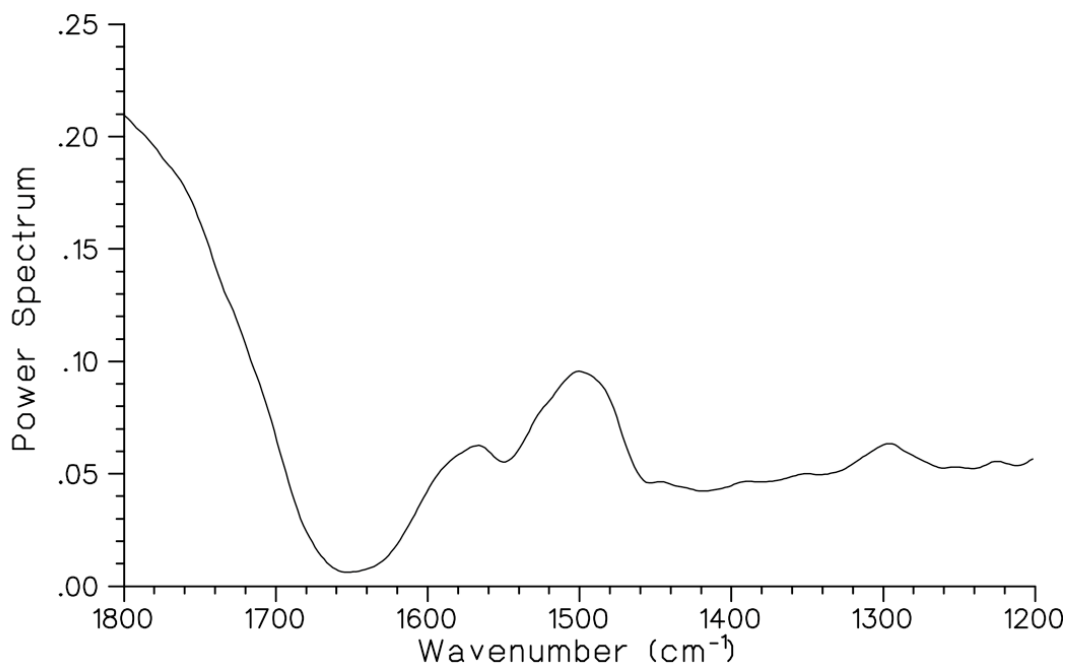


Figure 3.4: **30000 Scan Power Spectrum of PS I Sample.** The plot shows that very little light was getting through in the region of 1643 cm^{-1} , so a very small change produced the band in Figure 3.3.

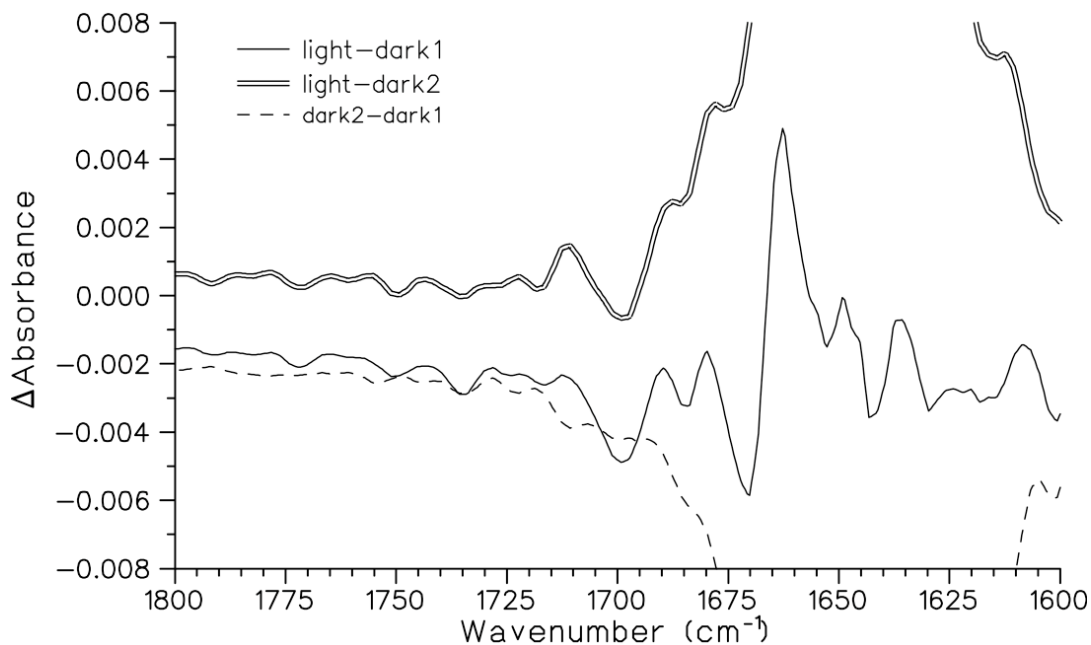


Figure 3.5: **30000 Scan PS I Light-Dark Spectra – Closer View of light-dark1**. Interesting bands similar to those obtained by Breton and Hastings appear at 1699 cm^{-1} , 1670 cm^{-1} and 1660 cm^{-1} .

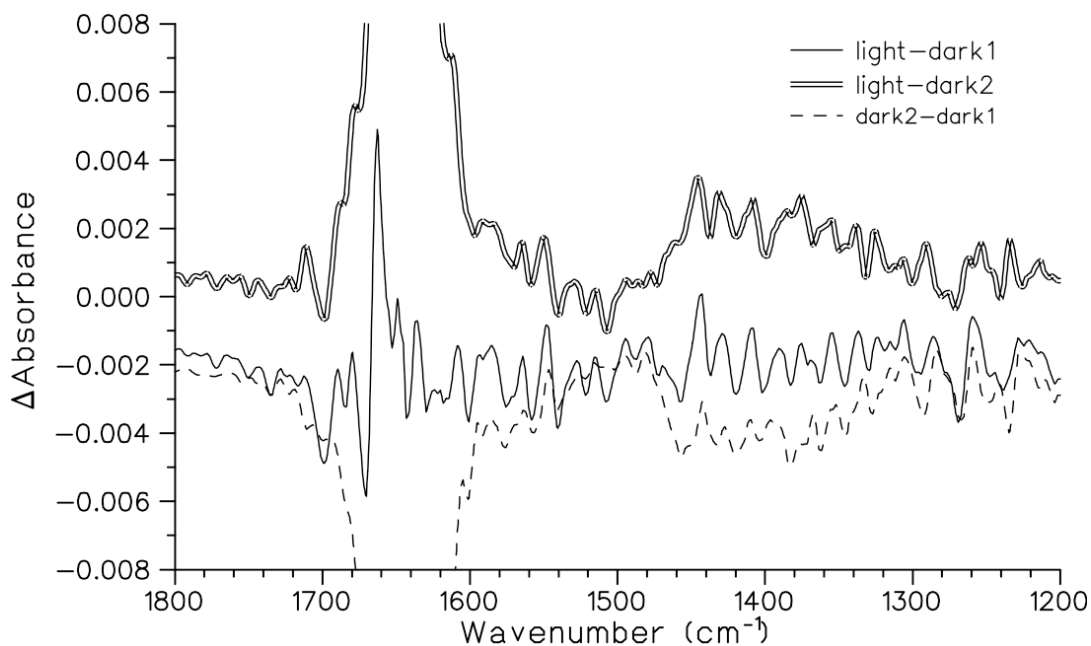


Figure 3.6: **30000 Scan PS I Light-Dark Spectra – Viewed to 1200 cm^{-1}** . The noise level between $1400\text{-}1500 \text{ cm}^{-1}$, where the spectra should be smooth, indicates that the data cannot really be trusted.

Chapter 4

Conclusions and Future Work

Hastings' spectra were not duplicated in the obtained light-dark results in a reliable way. The dark-dark spectral result shows that the data in the region of 1650 cm^{-1} cannot be trusted. The result of the light-dark1 spectrum was promising, however, and if the sample had been drier, the resultant spectrum may have shown the same light-dark signal as that of Hastings.

For comparison with Figure 3.3, a spectrum by Hastings that includes the dark-dark signal level is presented in Figure 4.1. Notably, the dark-dark signal on his plot is immeasurably small compared to the light-dark signal. The largest band of the light-dark signal at 1697.9 cm^{-1} has a magnitude of about 2×10^{-3} in terms of absorbance. This is comparable to the size of the noise (the bands of the dark-dark spectrum) shown in Figure 3.6. This means that further effort must be made to improve the signal-to-noise ratio.

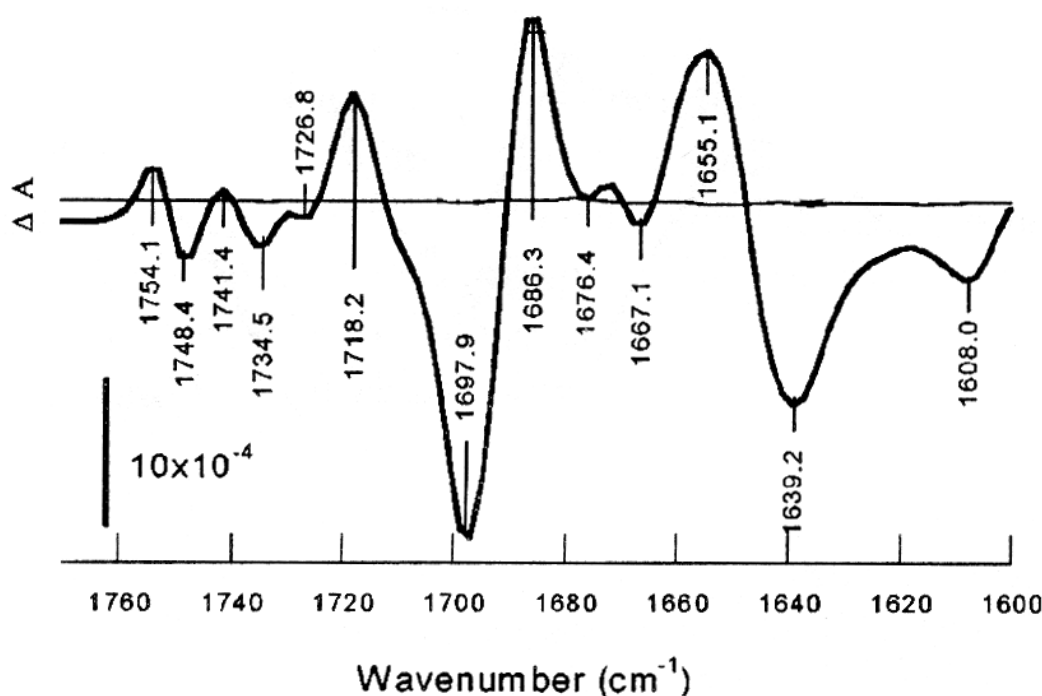


Figure 4.1: **Hastings PS I Spectrum Including Dark-Dark Reference.** The spectrum presented for PS I by Hastings. The dark-dark absorbance difference spectrum is shown to characterize the noise present.[13]

The most obvious way to improve the signal-to-noise ratio is through further signal averaging. This requires extending the scan times beyond those already employed. To achieve the three spectra (two dark and one light) presented in Figure 3.3, however, continuous scanning for 14 hours was performed. The data collection requires monitoring as the spectra were collected in a staggered order. Two people collecting the data on alternate shifts may be able to extend the scan times further. Increasing the scan frequency of the spectrometer should also be investigated.

The signal-to-noise ratio may also be improved by drying and concentrating the sample more. By removing more of the absorption due to water and putting more PS I particles in the light path, the desired signal should be more apparent. This could be accomplished by freeze drying the samples directly on one of the CaF_2 windows for an extended period such as several hours. The pelleting technique employed by Hastings may also be investigated.

A further method of increasing the signal may be to increase the actinic (laser) light source intensity. This could be accomplished by using a laser that is both more powerful and emits a frequency more strongly absorbed by PS I. An absorption spectrum for the visible range of PS II is shown in Figure 4.2. The absorbance spectrum for PS I is very similar, except that the lowest energy peak would appear at 700 nm, rather than 680 nm. The He-Ne laser used as an actinic source in this project emits at 632.8 nm.

Finally, spectra in the visible region should be performed to ensure the samples are healthy before and after obtaining IR spectra. A healthy PS I sample should show an absorption peak at 700 nm, since its reaction centre is P_{700} . Visible absorption spectra would also allow a direct comparison with Hastings' calibration, to ensure that the samples are concentrated enough to obtain a light-dark signal. He states that for his samples the peak at 678 nm had an absorption of 0.7-1.5.[12]

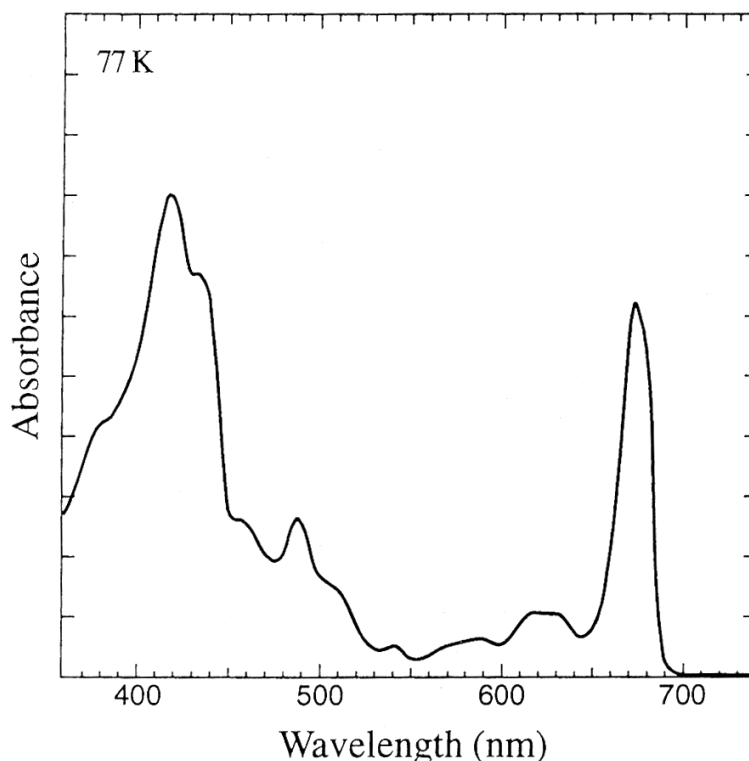


Figure 4.2: **PS II Visible Absorbance Spectrum.** The peak is observed at 680 nm since the reaction centre is P_{680} . The PS I reaction centre should show a similar peak at 700 nm.

Appendix A

Sample Physica Macro

This Physica macro produced the final light-dark difference spectra in Figure 3.3. The data was exported in data point table format, which produced two columns corresponding to wavenumber and power spectrum signal. The Physica scripting and plotting software may be obtained from <http://trshare.triumf.ca/~chuma/physica/homepage.html>.

```
device postscript
clear
defaults
orientation portrait
window 3
legend on
legend frame off
legend frame 20 70 40 90
legend nsymb 3

!read the data - note you can comment these lines for subsequent macro runs
read Bugs-in-CaF2-plates-w-N2-dark1-(10000).0.dat dark1_wavenumber0 dark1_powerspec0
read Bugs-in-CaF2-plates-w-N2-dark1-(10000).1.dat dark1_wavenumber1 dark1_powerspec1
read Bugs-in-CaF2-plates-w-N2-dark1-(10000).2.dat dark1_wavenumber2 dark1_powerspec2
read Bugs-in-CaF2-plates-w-N2-dark2-(10000).0.dat dark2_wavenumber0 dark2_powerspec0
read Bugs-in-CaF2-plates-w-N2-dark2-(10000).1.dat dark2_wavenumber1 dark2_powerspec1
read Bugs-in-CaF2-plates-w-N2-dark2-(10000).2.dat dark2_wavenumber2 dark2_powerspec2
read Bugs-in-CaF2-plates-w-N2-light-(10000).0.dat light_wavenumber0 light_powerspec0
read Bugs-in-CaF2-plates-w-N2-light-(10000).1.dat light_wavenumber1 light_powerspec1
read Bugs-in-CaF2-plates-w-N2-light-(10000).2.dat light_wavenumber2 light_powerspec2
read Two-CaF2-plates-ref-from-Aug-19.dat ref_wavenumber ref_powerspec

!add the trios for averaging
dark1_powerspec = (dark1_powerspec0+dark1_powerspec1+dark1_powerspec2)/3
dark2_powerspec = (dark2_powerspec0+dark2_powerspec1+dark2_powerspec2)/3
light_powerspec = (light_powerspec0+light_powerspec1+light_powerspec2)/3

!sort the data
sort dark1_wavenumber0 dark1_powerspec
sort dark2_wavenumber0 dark2_powerspec
sort light_wavenumber0 light_powerspec
sort ref_wavenumber ref_powerspec

!create the transmission spectra - make sure no division by zero
light_trans=light_powerspec/ref_powerspec
```

```
dark1_trans=dark1_powerspec/ref_powerspec
dark2_trans=dark2_powerspec/ref_powerspec

!take the negative logs to form the absorbance spectra - make sure no zero or -ve
light_absorbance = -log(light_trans)
dark1_absorbance = -log(dark1_trans)
dark2_absorbance = -log(dark2_trans)

!subtract to form the difference spectra
wavenumber=dark1_wavenumber0
absorbance_light_dark1=light_absorbance-dark1_absorbance
absorbance_light_dark2=light_absorbance-dark2_absorbance
absorbance_dark1_dark2=dark2_absorbance-dark1_absorbance

!make a smooth function to plot
generate smooth_wav 500 , , 3500 6000
set tension 25
interp_abs_light_dark1 = interp(wavenumber,absorbance_light_dark1,smooth_wav)
interp_abs_light_dark2 = interp(wavenumber,absorbance_light_dark2,smooth_wav)
interp_abs_dark1_dark2 = interp(wavenumber,absorbance_dark1_dark2,smooth_wav)

set LINTHK 1.0

!Lower Corner
set cursor -1
set %txthit 0.1
set %xloc 3
set %yloc 4
text '.'
!Upper Corner
set %xloc 97.5
set %yloc 92
text '.'

set LINTHK 4.0

!scales and axes
!Sometimes physica gets confused and doesn't draw the x-axis scale:
!make sure specify nlxinc and nlyinc (6 and 8 in this example)
set box 0
scales 1800 1600 6 -0.008 0.008 8
set %xlabsz 3
set %xnumsz 2.5
set %ylabsz 3
set %ynumsz 2.5
set nsxinc 5
set nsyinc 2
```

```
lab\x '<Fhelvetica.1>Wavenumber (cm<^-1<_>)'
lab\y '<Fhelvetica.1><Delta>Absorbance'
graph\axesonly smooth_wav interp_abs_light_dark1

set LINTHK 3.0

!graph the smoothed function
set pchar 0
set LINTYP 1
graph\noax 'light-dark1' smooth_wav interp_abs_light_dark1
set LINTYP 2
graph\noax 'light-dark2' smooth_wav interp_abs_light_dark2
set LINTYP 7
graph\noax 'dark2-dark1' smooth_wav interp_abs_dark1_dark2
```

Appendix B

Table of Absorptions

Wavenumber (cm ⁻¹)	Bond	Mode	Remarks
667	C=O	Bending	Atmospheric CO ₂
1020-1220	C-N	Stretching	PS I Sample
1280-2000	O-H	Unknown	H ₂ O (moist atmosphere)
1425	C-H	Bending	Polypropylene
1643	O-H	Bending	Liquid water in sample
1650	C=O	Stretching	PS I sample
2345	C=O	Asymmetric stretch	Atmospheric CO ₂
2850-2975	C-H	Stretching	Polypropylene and PS I samples
3330-3450	O-H	Symmetric and asymmetric stretch	Liquid water in sample

Table B.1: **Compilation of Identified IR Bands.** List of the identified absorption bands that appeared in the spectra presented in this paper.[10, 16, 22]

Bibliography

- [1] Physics 3P93: Photoconductivity. Course notes, Physics Department, Brock University, 2004.
- [2] B. A. Barry, S. Kim, C. A. Sacksteder, and K. A. Bixby. A Reaction-Induced FT-IR Study of Cyanobacterial Photosystem I. *Biochemistry*, 40:15384–15395, 2001.
- [3] J. Breton, E. Nabedryk, and W. Leibl. FTIR Study of the Primary Electron Donor of Photosystem I (P700) Revealing Delocalization of the Charge in P700⁺ and Localization of the Triplet Character in ³P700. *Biochemistry*, 38(36):11585–11592, 1999.
- [4] Jacques Breton. Fourier Transform Infrared Spectroscopy of Primary Electron Donors in Type I Photosynthetic Reaction Centres. *Biochimica et Biophysica Acta (BBA) / Bioenergetics*, 1507(1-3):180–193, 2001.
- [5] J.L. Chuma. Physica Online Documentation. TRIUMF: <http://trshare.triumf.ca/~chuma/physica/homepage.html>.
- [6] N.B. Colthup, L.H. Daly, and S.E. Wiberly. *Introduction to Infrared and Raman Spectroscopy*. Academic Press, 3 edition, 1990.
- [7] S. Debnath, E. Jiang, and J. Coffin. Performance Characteristics of the Advanced ETC EverGlo IR Source. Thermo Electron Corporation, 2007. http://www.thermo.com/eThermo/CMA/PDFs/Articles/articlesFile_24227.pdf.
- [8] S.A. Dodds. Notes on Noise Reduction. Phys 331 course laboratory manual, Department of Physics and Astronomy, Rice University, 2007.
- [9] Gunzler and Williams, editors. *Handbook of Analytical Techniques*, volume 1. Wiley VCH, New York, 2001.
- [10] H. Günzler and H.-V. Gremlich. *IR Spectroscopy: An Introduction*. Wiley-VCH, Weinheim, 2002.
- [11] D.O. Hall and K.K. Rao. *Photosynthesis*, 5th ed. Cambridge University Press, New York, 1994.
- [12] G. Hastings. Time-Resolved Step-Scan Fourier Transform Infrared and Visible Absorption Difference Spectroscopy for the Study of Photosystem I. *Applied Spectroscopy*, 55(7):894–900, 2001.
- [13] G. Hastings, V. M. Ramesh, R. Wang, V. Sivakumar, and A. Webber. Primary Donor Photo-Oxidation in Photosystem I: A Re-Evaluation of (P700⁺ - P700) Fourier Transform Infrared Difference Spectra. *Biochemistry*, 40:12943–12949, 2001.
- [14] G. Hastings, R. Wang, V. Sivakumar, and T. W. Johnson. FTIR Difference Spectroscopy in Combination with Isotope Labeling for Identification of the Carbonyl Modes of P700 and P700⁺ in Photosystem I. *Biophysical Journal*, 86:1061–1073, 2004.

-
- [15] E.R. Leadbetter II and J.S. Poindexter, editors. *Bacteria in Nature, Volume 1*. Plenum Press, New York, 1985.
- [16] Yun Hee Jang. Infrared Spectroscopy. CalTech Materials and Process Simulation Center: <http://www.wag.caltech.edu/home/jang/genchem/infrared.htm>.
- [17] Purves, Orians, Heller, and Sadan. *Life, The Science of Biology 5th ed.* WH Freeman & Associates, Salt Lake City, 1998.
- [18] H. E. Shubeita. Basic Lab Knowledge and Skills. Dept of Chemistry, San Diego State University: <http://www.sci.sdsu.edu/classes/chemistry/chem4671/shubeita/labskills.htm>.
- [19] B. Stuart. *Infrared Spectroscopy: Fundamentals and Applications*. Wiley, Hoboken, NJ, 2004.
- [20] Janos Technology. Optical Material Selection Guide. <http://www.janostech.com>.
- [21] A. van der Est. Interview. Brock University, 2004.
- [22] S.Y. Venyaminov and F.G. Prendergast. Water (H₂O and D₂O) Molar Absorptivity in the 1000-4000 cm⁻¹ Range and Quantitative Infrared Spectroscopy of Aqueous Solutions. *Analytical Biochemistry*, 248:234–245, 1997.
- [23] D. Walker. *Energy, Plants and Man, 2nd ed.* Oxygraphics, Limited, Brighton, 1992.